Physical Processes Associated with Heavy Flooding Rainfall in Nashville, Tennessee, and Vicinity during 1–2 May 2010: The Role of an Atmospheric River and Mesoscale Convective Systems*

BENJAMIN J. MOORE

Cooperative Institute for Research in Environmental Sciences, University of Colorado, and NOAA/Earth System Research Laboratory, Boulder, Colorado

PAUL J. NEIMAN AND F. MARTIN RALPH

NOAA/Earth System Research Laboratory/Physical Sciences Division, Boulder, Colorado

FAYE E. BARTHOLD

I. M. Systems Group, Inc., and NOAA/Hydrometeorological Prediction Center, Camp Springs, Maryland

(Manuscript received 27 May 2011, in final form 24 August 2011)

ABSTRACT

A multiscale analysis is conducted in order to examine the physical processes that resulted in prolonged heavy rainfall and devastating flash flooding across western and central Tennessee and Kentucky on 1–2 May 2010, during which Nashville, Tennessee, received 344.7 mm of rainfall and incurred 11 flood-related fatalities. On the synoptic scale, heavy rainfall was supported by a persistent corridor of strong water vapor transport rooted in the tropics that was manifested as an atmospheric river (AR). This AR developed as water vapor was extracted from the eastern tropical Pacific and the Caribbean Sea and transported into the central Mississippi Valley by a strong southerly low-level jet (LLJ) positioned between a stationary lee trough along the eastern Mexico coast and a broad, stationary subtropical ridge positioned over the southeastern United States and the subtropical Atlantic. The AR, associated with substantial water vapor content and moderate convective available potential energy, supported the successive development of two quasi-stationary mesoscale convective systems (MCSs) on 1 and 2 May, respectively. These MCSs were both linearly organized and exhibited back-building and echo-training, processes that afforded the repeated movement of convective cells over the same area of western and central Tennessee and Kentucky, resulting in a narrow band of rainfall totals of 200–400 mm. Mesoscale analyses reveal that the MCSs developed on the warm side of a slow-moving cold front and that the interaction between the southerly LLJ and convectively generated outflow boundaries was fundamental for generating convection.

1. Introduction

a. Event overview

During 1–2 May 2010, two successive quasi-stationary mesoscale convective systems (MCSs; Fig. 1) produced historic 48-h (0000 UTC 1 May–0000 UTC 3 May) rainfall accumulations across western and central Tennessee and Kentucky that ranged from 200 to >400 mm (344.7 mm at Nashville; Fig. 2), exceeding the 1000-yr recurrence interval for 48-h rainfall totals at many locations (National Weather Service 2011, hereafter NWS11). The heavy rainfall produced during the life spans of the two MCSs (~0600 UTC 1 May–0000 UTC 2 May and ~0900 UTC 2 May–0000 UTC 3 May, respectively) resulted in devastating flooding throughout the Cumberland River and Tennessee River basins of Tennessee and Kentucky, with all-time record water levels and discharges observed at several river gauging sites (NWS11). The Nashville, Tennessee, metropolitan area was heavily impacted by flooding of the Cumberland

* Supplemental information related to this paper is available at the Journals Online Web site: http://dx.doi.org/10.1175/MWR-D-11-00126.s1.

Corresponding author address: Benjamin J. Moore, Physical Sciences Division, NOAA/Earth System Research Laboratory, Mail Code R/PSD2, 325 Broadway, Boulder, CO 80305.
E-mail: benjamin.moore@noaa.gov

DOI: 10.1175/MWR-D-11-00126.1

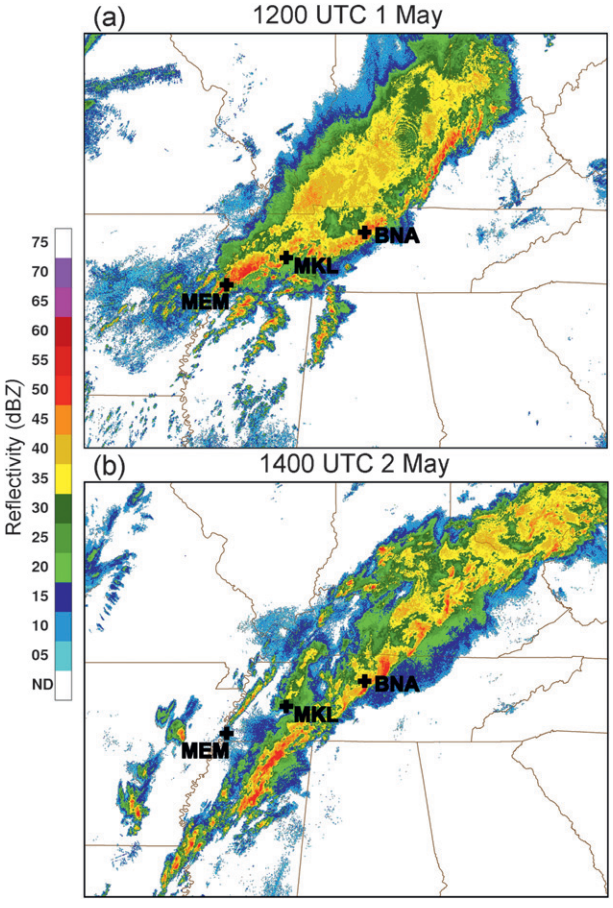

FIG. 1. National Mosaic and Multisensor QPE project composite reflectivity imagery (shaded in dBZ) depicting (a) the first MCS at 1200 UTC 1 May 2010 and (b) the second MCS at 1400 UTC 2 May 2010. For reference, the locations of Memphis (MEM), Jackson (MKL), and Nashville (BNA) in TN are denoted.

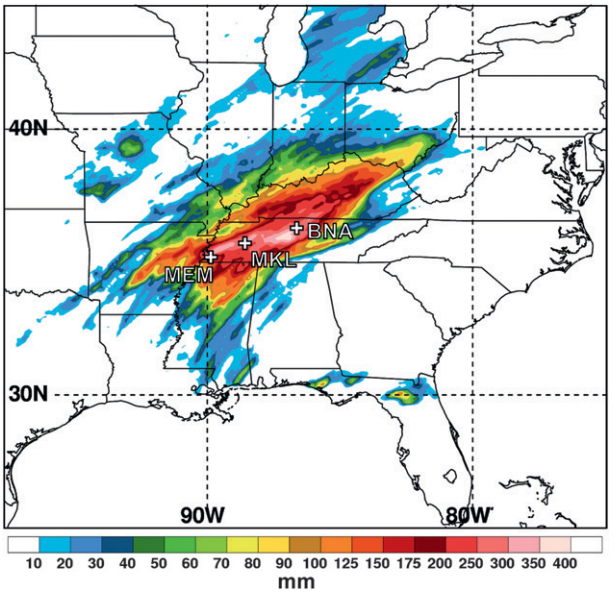

FIG. 2. Total accumulated precipitation (shaded in mm according to the color bar) from the National Precipitation Verification Unit quantitative precipitation estimates product for 0000 UTC 1 May–0000 UTC 3 May 2010. The locations of Memphis, Jackson, and Nashville in TN are denoted as in Fig. 1.

River and its tributaries, incurring 11 fatalities and nearly $2 billion in damages to infrastructure and property (NWS11). In total, flooding resulted in 26 fatalities and caused $2–$3 billion in damages throughout Tennessee and Kentucky during 1–4 May (NWS11).

A distinguishing aspect of this high-impact extreme rainfall event was that it was linked to the formation and persistence of a conspicuous narrow plume of enhanced vertically integrated water vapor (IWV), depicted in Figs. 3a–d and in the supplemental material, that extended into the central Mississippi Valley from a tropical IWV reservoir (values of 65–75 mm) over the eastern tropical Pacific near Central America. These IWV observations are illustrative of possible direct water vapor transport from the tropics into the heavy rain region of Tennessee and Kentucky during 1–2 May, with potential water vapor contributions from the eastern tropical Pacific and from, as suggested by Higgins et al. (2011), the Caribbean Sea. Furthermore, the narrow structure of the enhanced IWV plume stretching poleward from the tropics suggests that water vapor transport was concentrated within a narrow corridor or, specifically, an ''atmospheric river'' (AR; e.g., Newell et al. 1992; Zhu and Newell 1998; Ralph et al. 2004).

Atmospheric rivers have received considerable attention in the scientific literature in relation to extratropical cyclones over open ocean basins and to heavy precipitation along the western coasts of continents; however, very few studies have focused on ARs over the central United States and their possible role in producing heavy rainfall therein. Given this relative gap in research related to central U.S. ARs and given the extreme rainfall and catastrophic flooding in Tennessee and Kentucky during 1–2 May 2010, this paper examines the AR event of 1–2 May 2010 with specific focus on diagnosing 1) the synoptic-scale processes and flow features facilitating water vapor transport from the tropics into the central Mississippi Valley, and 2) the role of the AR in producing nearly continuous heavy convective rainfall over a 2-day period. Within the latter component, the mesoscale conditions and physical mechanisms that served to focus heavy rainfall along a relatively narrow corridor in Tennessee and Kentucky during 1–2 May will be investigated. This mesoscale investigation is crucial because, despite operational forecasters' recognition of the potential for heavy rainfall and flash flooding throughout the central Mississippi

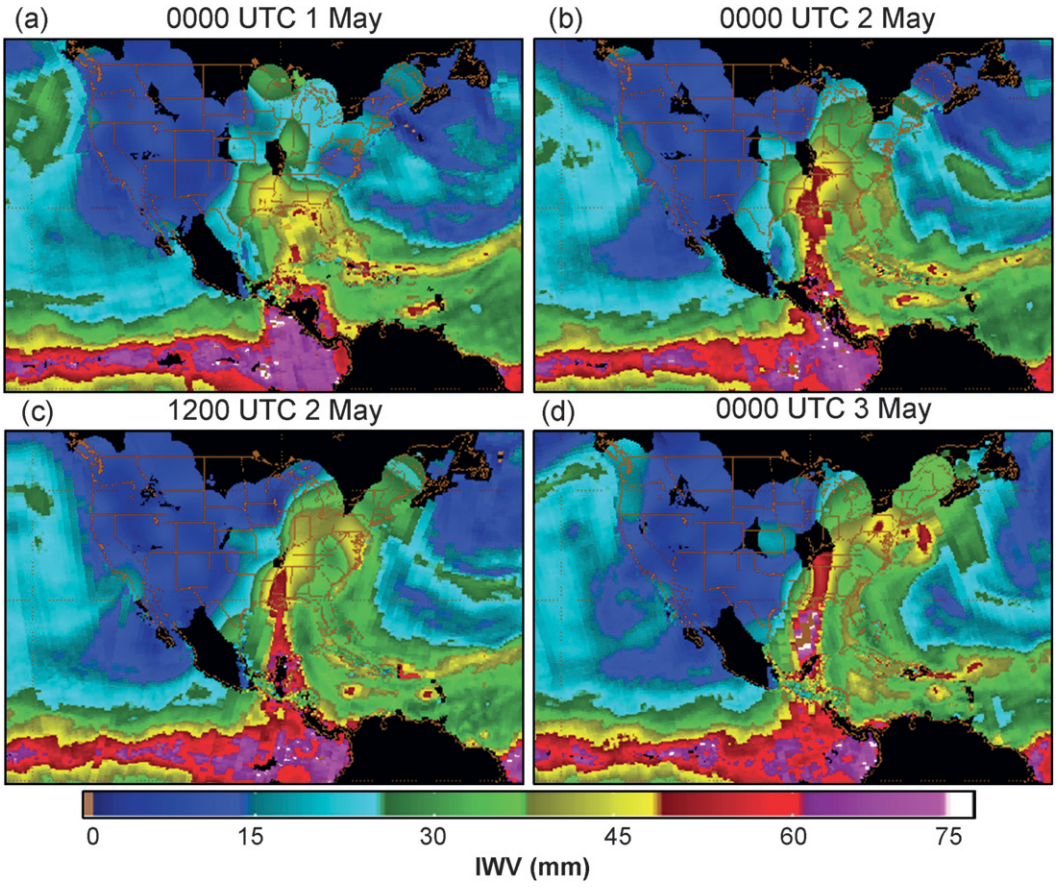

FIG. 3. NOAA/NESDIS blended IWV imagery (shaded in mm according to the color bar) for (a) 0000 UTC 1 May, (b) 0000 UTC 2 May, (c) 1200 UTC 2 May, and (d) 0000 UTC 3 May 2010.

Valley region during 1–2 May several days in advance of this event, the magnitude of the extreme rainfall totals and the spatially focused nature of the rainfall distribution across Tennessee and Kentucky (Fig. 2) were not well anticipated (NWS11).

b. Linkage between tropical water vapor and heavy precipitation at midlatitudes

Poleward transports of water vapor from the tropics contributing to heavy precipitation at midlatitudes typically occur in connection with meso-alpha-scale and synoptic-scale weather systems, such as extratropical cyclones (e.g., Lackmann and Gyakum 1999; Neiman et al. 2008a,b; Ralph et al. 2011), slow-moving subtropical lows (e.g., Knippertz and Martin 2005, 2007), and tropical cyclones (e.g., Bosart and Carr 1978; Higgins et al. 2004; Stohl et al. 2008; Galarneau et al. 2010). Over the North Pacific and North Atlantic Ocean basins, tropical water vapor transports are frequently facilitated by ARs (e.g., Zhu and Newell 1998). These ARs typically form in connection with the precold-frontal low-level jet (LLJ) located within the warm sectors of transient maritime extratropical cyclones (e.g., Ralph et al. 2004), constituting a narrow substructure of the broad "warm conveyor belt" (e.g., Browning 1990; Carlson 1991). When ARs make landfall in regions of steep mountainous terrain, such as the western coast of North America, strong and concentrated upslope water vapor flux, in the presence of weak static stability and large water vapor content (IWV values >20 mm), can produce heavy orographic precipitation and flooding (e.g., Ralph et al. 2003, 2004, 2005, 2006; Neiman et al. 2008a,b, 2011; Stohl et al. 2008; Smith et al. 2010; Ralph and Dettinger 2011).

In a scenario that has classically been referred to as the "Pineapple Express" (e.g., Lackmann and Gyakum 1999; Dettinger 2004; Dettinger et al. 2011), ARs over the eastern North Pacific contributing to heavy precipitation along the west coast of North America can exhibit a direct connection to a tropical Pacific water vapor reservoir near the Hawaiian Islands (e.g., Bao et al. 2006; Neiman et al. 2008a,b; Ralph et al. 2011). Though they did not apply the AR terminology, Knippertz

and Martin (2007) documented the important role of a quasi-stationary midlevel cutoff low over the eastern subtropical Pacific for transporting water vapor at midlevels from the tropics into the southwestern United States, fueling widespread heavy precipitation in an otherwise arid region. For the North Atlantic, Stohl et al. (2008) documented the role of an AR associated with two former hurricanes undergoing extratropical transition in transporting water vapor from the tropical Atlantic to the western coast of Norway, contributing to extreme orographically forced precipitation near the city of Bergen, Norway. Additionally, Halverson and Rabenhorst (2010) suggested that an AR rooted in the tropics contributed to a high-impact heavy snowfall event during 5–6 February 2010 in the mid-Atlantic region of the United States.

Numerous studies have discussed the important linkage between water vapor transported from the Gulf of Mexico and the Caribbean Sea and heavy rainfall in the central United States (e.g., Benton and Estoque 1954; Bell and Janowiak 1995; Trenberth and Guillemot 1996; Higgins et al. 1997, 2011; Dirmeyer and Kinter 2009, 2010; Knippertz and Wernli 2010). On synoptic scales, this linkage, recently dubbed the ''Maya Express'' by Dirmeyer and Kinter (2009) and discussed in detail by Dirmeyer and Kinter (2010), is typically established when moist low-level air originating within the planetary boundary layer (PBL) over the Caribbean Sea and the Gulf of Mexico is transported westward and poleward by anticyclonic low-level flow on the periphery of a persistent subtropical ridge positioned over the southeastern United States and the subtropical Atlantic. Upon reaching the Gulf of Mexico coast, this moist air is transported rapidly poleward into the central United States by a southerly LLJ, eventually producing heavy rainfall when it is forced to ascend.

Transports of water vapor from the tropics into the central United States can occur in connection with ARs. However, owing to the complex physical geography of the North American continent and its impacts on the development of synoptic-scale weather systems (e.g., Hobbs et al. 1996), the synoptic-scale flow configurations and processes associated with central U.S. ARs likely differ from those associated with ''classic'' precold-frontal ARs over open-ocean basins. Specifically, in the spring and early summer, southerly LLJs that support water vapor transport into the central United States commonly develop in connection with a strong low-level pressure (or geopotential height) gradient between a developing terrain-induced lee trough or extratropical cyclone to the east of the Rocky Mountains and a subtropical ridge over the southeastern United States and may not involve a well-defined surface cold front (e.g., Djurić and Damiani 1980; Uccellini 1980; Augustine and Howard 1991; Martin et al. 1995; Mo et al. 1995).

When moist tropical air is drawn poleward from the Gulf of Mexico and the Caribbean Sea into the central United States by a southerly LLJ, large tropospheric water vapor content combined with large convective available potential energy (CAPE) can often support deep moist convection. Locally extreme rainfall can result when deep moist convection is anchored over a location for a prolonged period of time, a scenario that commonly occurs in association with quasi-stationary MCSs (e.g., Chappell 1986; Doswell et al. 1996; Schumacher and Johnson 2005). Quasi-stationary heavy-rain-producing MCSs often develop when a stream of warm, moist, and unstable (i.e., large CAPE) air, advected by an LLJ, impinges upon a quasi-stationary low-level mesoscale baroclinic zone (e.g., frontal boundary, convectively generated outflow boundary), producing the requisite lift, water vapor convergence, and thermodynamic destabilization to continuously generate convection (e.g., Maddox et al. 1979; Chappell 1986; Trier and Parsons 1993; Junker et al. 1999; Moore et al. 2003; Schumacher and Johnson 2005).

c. *Organization of paper*

The remainder of this paper is organized as follows. Section 2 provides an overview of the key datasets used for analysis. Section 3 discusses the evolution of the synoptic-scale conditions over North America during 1–2 May 2010. The physical processes supporting heavy rainfall are diagnosed in section 4. Last, section 5 provides the synthesis and conclusions.

2. Key datasets

The multiscale analysis in the present study draws upon a variety of observational and numerical model-based datasets. Observational datasets include the following: (i) National Precipitation Verification Unit (NPVU; http://www.hpc.ncep.noaa.gov/npvu/) quantitative precipitation estimates (QPE) product (McDonald and Baker 2001) gridded at 4-km horizontal resolution, (ii) national composite radar reflectivity mosaics from the National Mosaic and Multisensor QPE project (Vasiloff et al. 2007), (iii) Weather Surveillance Radar-1988 Doppler (WSR-88D) base reflectivity mosaics archived at the State University of New York at Albany, (iv) hourly Automated Surface Observing System observations and twice-daily radiosonde observations (obtained from the Iowa State University Department of Agronomy online data archive; http://mesonet.agron.iastate.edu/archive/), (v) National Oceanic and Atmospheric Administration

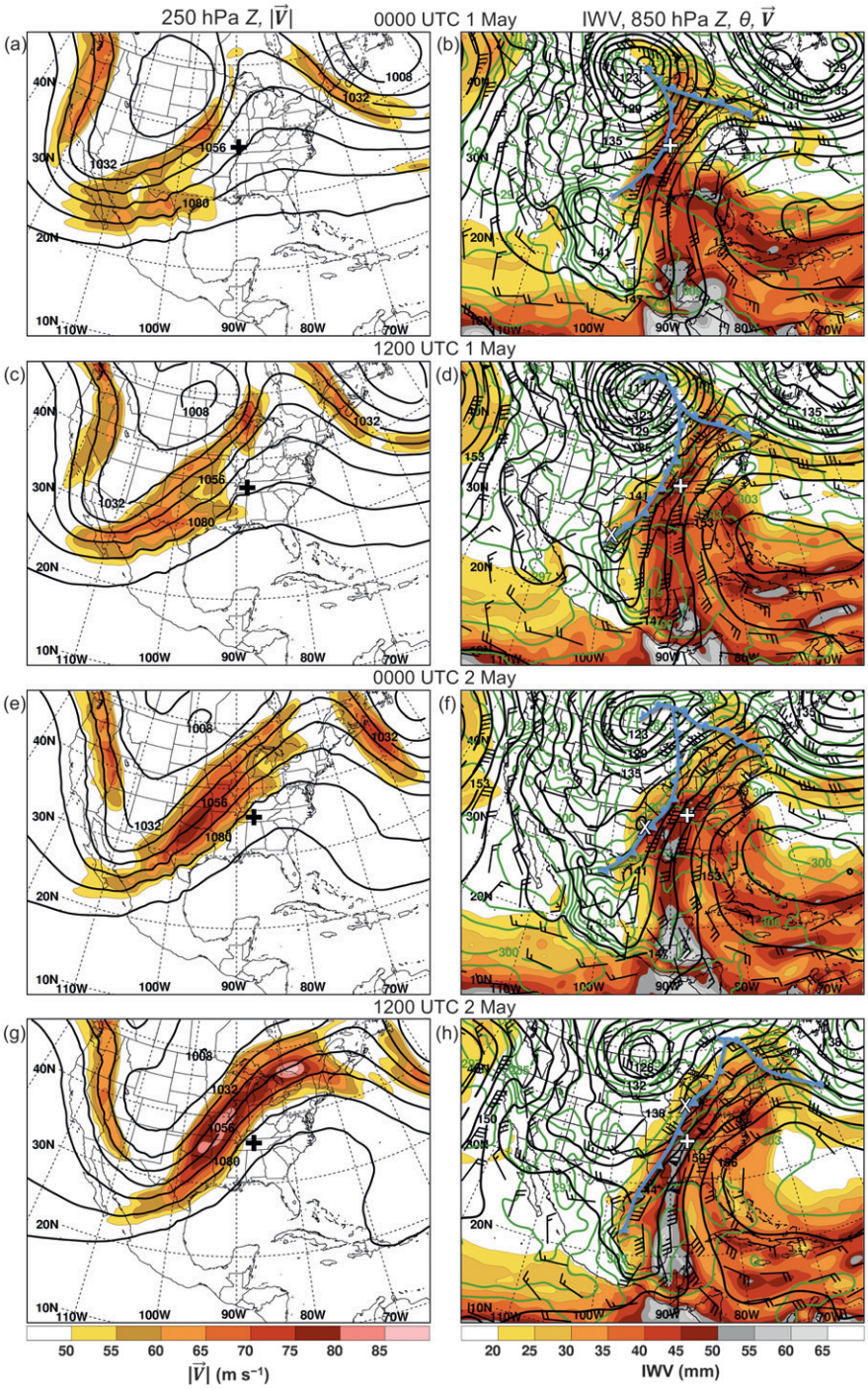

FIG. 4. (a),(c),(e),(g) 250-hPa geopotential height (contoured in black every 10 dam) and wind speed (shaded in m s^{-1} according to the color bar). (b),(d),(f),(h) IWV (shaded in mm according to the color bar) and 850-hPa geopotential height (contoured in black every 3 dam), potential temperature (contoured in green every 3 K), and wind (plotted for wind speeds $\geq$5 m s^{-1}, half barb: 2.5 m s^{-1}; full barb: 5 m s^{-1}; pennant: 25 m s^{-1}). Manually analyzed positions of the surface fronts are drawn in blue in standard frontal notation in (b),(d),(f),(h); and the position of the frontal wave described in the text is marked by an "×" symbol in (d),(f), and (h). The MCS location is denoted in each by the "+" symbol. Plots were generated from the 0.5° GFS analyses at (a),(b) 0000 UTC 1 May; (c),(d) 1200 UTC 1 May; (e),(f) 0000 UTC 2 May; and (g),(h) 1200 UTC 2 May 2010.

(NOAA)/National Environmental Satellite, Data, and Information Service (NESDIS) blended satellite IWV imagery (Kidder and Jones 2007), and (vi) Cooperative Institute for Meteorological Satellite Studies (CIMSS) Morphed Integrated Microwave Imagery at CIMSS (MIMIC) IWV imagery. Wind profiler observations from the NOAA Profiler Network site at Okolona, Mississippi, were unavailable for 1–3 May 2010.

The National Centers for Environmental Prediction (NCEP) Global Forecast System (GFS) 6-h model analyses with 0.5° × 0.5° horizontal and 50-hPa (25 hPa between 1000 and 900 hPa) vertical resolution were used to generate synoptic-scale charts and to perform diagnostic calculations. Some mesoscale charts and diagnostics were generated using the Rapid Update Cycle (RUC) hourly model analyses (Benjamin et al. 2004) with 13-km horizontal and 25-hPa vertical resolution. For select analysis times, normalized anomaly fields were generated from the NCEP GFS analyses, using, as in Hart and Grumm (2001), the 21-day running long-term (1979–2008) mean and standard deviation values, centered on the day being investigated, that were computed from the 2.5° NCEP–National Center for Atmospheric Research (NCEP–NCAR) reanalysis dataset (Kalnay et al. 1996).[1] Backward air parcel trajectories were computed from the NCEP Global Data Assimilation System (GDAS) 6-h model analyses, with 1° × 1° horizontal and 50-hPa (25 hPa between 1000 and 900 hPa) vertical resolution, using the NOAA Hybrid Single-Particle Lagrangian Integrated Trajectory (HYSPLIT) model (Draxler and Hess 1997; Draxler and Rolph 2011).

3. Synoptic overview

a. Conditions during 1–2 May 2010

At 0000 UTC 1 May, a deep positively tilted 250-hPa trough was situated over southwestern North America upstream of closed low associated with a deep occluded cyclone over the northern plains (Figs. 4a,b). To the east of the northern plains cyclone, a prominent 250-hPa ridge was in place across the eastern United States and eastern Canada (Fig. 4a), flanked to the southeast by a broad 850-hPa ridge centered over the subtropical Atlantic (Fig. 4b). To the southeast of the 250-hPa trough over southwestern North America, deep tropospheric southwesterly flow (not shown) beneath a relatively diffuse 250-hPa jet streak (Fig. 4a) extended across the high terrain of the Mexican Plateau (see Fig. 8a for terrain

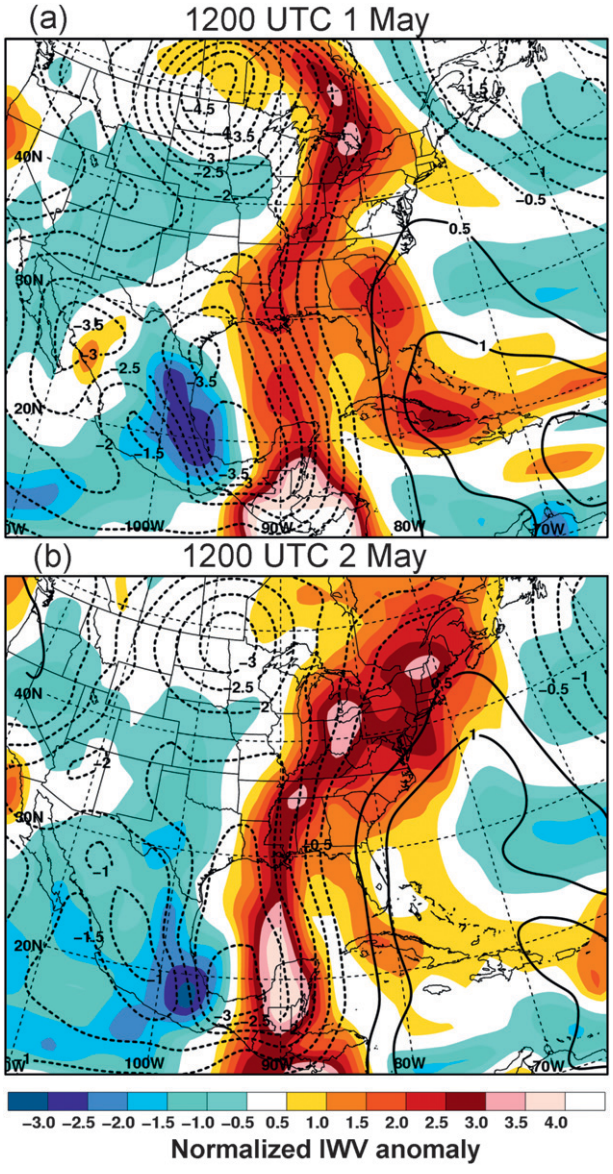

FIG. 5. Normalized anomalies of IWV (standard deviation values shaded according to the color bar) and 850-hPa geopotential height (contoured every 0.5 standard deviations with negative values shown in the dashed contours) for (a) 1200 UTC 1 May and (b) 1200 UTC 2 May 2010. The computation of the anomalies is described in the text.

map), the Gulf of Mexico, and the southern United States. An 850-hPa lee trough was positioned along the eastern Mexico coast from the Texas–Mexico border to Central America (Fig. 4b), likely linked to downslope flow (not shown) along the Sierra Madre Oriental Mountains of eastern Mexico. An anticyclonically curved corridor of strong poleward 850-hPa flow (hereafter the LLJ), corresponding to a plume of water vapor with IWV values of 30–55 mm, extended from Central America across the Gulf of Mexico to the Great Lakes in association with

[1] The resolution mismatch between the 0.5° GFS and the 2.5° NCEP–NCAR datasets may yield normalized anomaly values that are artificially large, but that are still qualitatively useful.

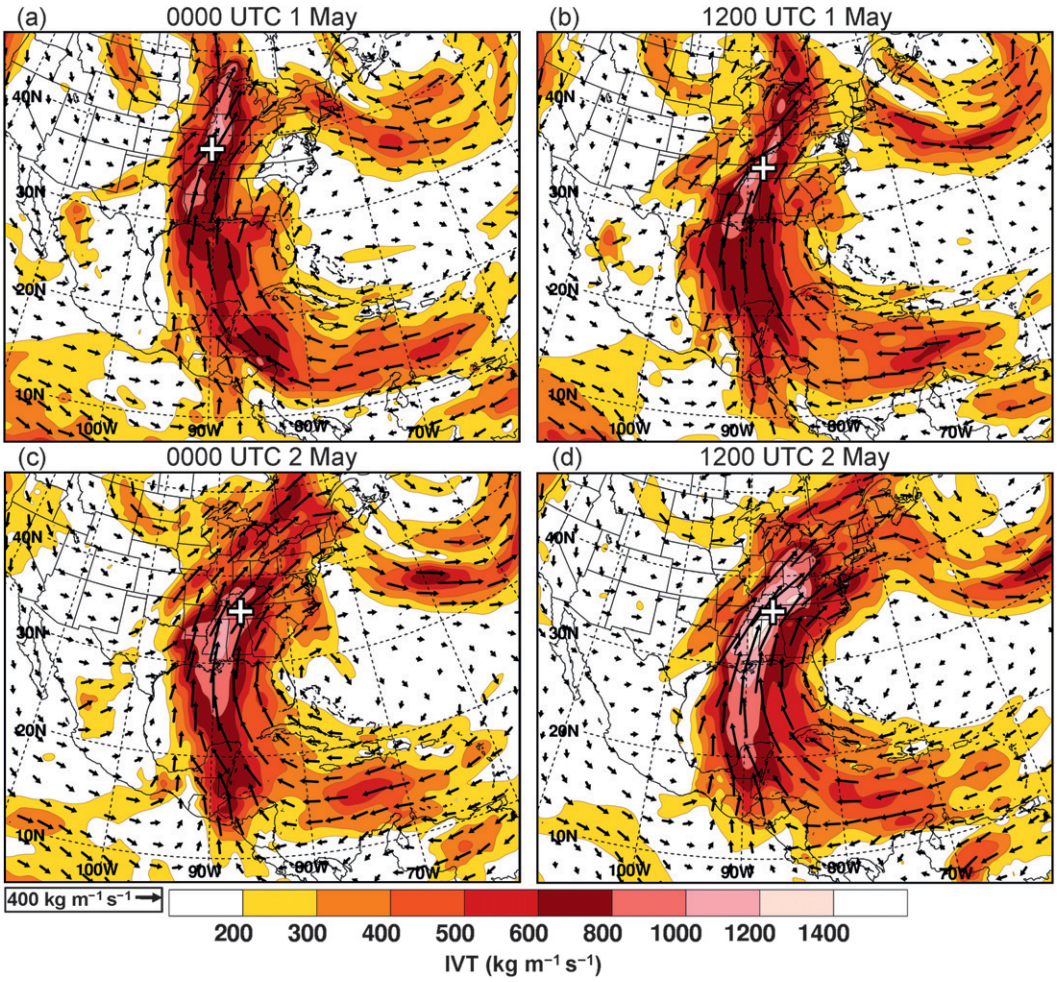

FIG. 6. 1000–300-hPa IVT (shaded in kg m^{-1} s^{-1} with vectors overlaid; vector scale is shown at bottom left) generated from the 0.5° GFS analyses at (a) 0000 UTC 1 May, (b) 1200 UTC 1 May, (c) 0000 UTC 2 May, and (d) 1200 UTC 2 May 2010. The MCS location is denoted in each by the "+" symbol.

a strong geopotential height gradient between the lee trough and the subtropical ridge and with a strong geopotential height gradient in the warm sector of the northern plains cyclone (Fig. 4b). Warm advection was evident along the axis of the LLJ over the Gulf of Mexico and the south-central United States to the east of the cold front trailing from the northern plains cyclone (Fig. 4b).

Through the subsequent 36 h, during which the two MCSs developed, the 250-hPa trough progressed slowly southeastward across the southwestern United States and northern Mexico, while the 250-hPa ridge over the eastern United States and eastern Canada amplified and remained generally stationary (Figs. 4a,c,e,g). Ahead of the trough, the southwesterly 250-hPa jet streak strengthened and shifted northeastward from northern Mexico into the central United States (Figs. 4a,c,e,g). The two MCSs were positioned beneath the equatorward jet exit region and the anticyclonic shear side of the jet core (Figs. 4c,g), respectively, and not beneath regions typically favorable for jet-related forcing of ascent (e.g., Uccellini and Johnson 1979). At 850 hPa, the lee trough and the subtropical ridge remained stationary during 1–2 May, maintaining strong poleward flow (i.e., the LLJ) across Central America, the Gulf of Mexico, and the south-central United States (Figs. 4b,d,f,h).

During 1–2 May, the LLJ maintained warm advection over the Gulf of Mexico and south-central United States, corresponding to weak quasigeostrophic forcing for ascent in the lower troposphere as diagnosed from calculations of **Q**-vector convergence (e.g., Hoskins et al. 1978; not shown), and contributed to a steady poleward stream of water vapor (IWV values 45–60 mm) from a tropical IWV reservoir near Central America, across the Gulf of Mexico, and into the environments of the two MCSs (Figs. 4b,d,f,h). During the time period, the MCSs were positioned along the

axis of the LLJ to the east of the trailing cold front, which was essentially stationary across the central United States (Figs. 4b,d,f,h). By 1200 UTC 2 May, a contiguous narrow band of IWV values exceeding 50 mm extended from the Yucatan Peninsula into the environment of the second MCS over western Tennessee (Fig. 4h). The development of this narrow band of large IWV coincided with an enhancement of confluence and a local acceleration of winds from 15–20 to 25–30 m s^{-1} at 850 hPa across Mississippi, Alabama, Tennessee, and Kentucky (Figs. 4d,f,h) accompanying the passage of a mesoscale frontal wave (labeled "×" in Figs. 4d,f,h) across the central Mississippi Valley.

By 0000 UTC 3 May (not shown), the second MCS had begun to move eastward as the upstream 250-hPa trough progressed into the central plains. Low-level cold advection had developed across the central Mississippi Valley, causing the cold front to advance eastward across the region. The axis of large IWV had begun to shift eastward ahead of the cold front and the associated 250-hPa trough, giving way to much drier tropospheric conditions and generally signaling the dissipation of convection across western and central Tennessee and Kentucky.

b. *Anomalous synoptic-scale conditions*

To provide perspective on the anomalous nature of the synoptic-scale conditions over North America relative to climatology during 1–2 May 2010, normalized anomalies of 850-hPa geopotential height and IWV are presented in Fig. 5 for 1200 UTC 1 May and 1200 UTC 2 May. For both analysis times, the lee trough along the eastern Mexico coast was associated with 850-hPa geopotential height anomalies in excess of 3 standard deviations below the climatological mean, while the subtropical ridge centered over the Atlantic was associated with anomalies exceeding 1.0 standard deviation above the mean through a large region over the western Atlantic, the Caribbean Sea, and the southeastern United States, with the areal coverage of positive anomalies increasing from 1 to 2 May. The juxtaposition of these negative and positive 850-hPa geopotential height anomalies established an anomalous geopotential height gradient and a corridor of anomalous poleward 850-hPa geostrophic flow (i.e., the LLJ) across the Gulf of Mexico and south-central United States.

At 1200 UTC 1 May, IWV anomalies of 1.5–2.5 standard deviations above the mean extended from the Yucatan Peninsula into the central Mississippi Valley (Fig. 5a). A notable feature at 1200 UTC 1 May was a large region of IWV anomalies ranging from 2.5 to well over 4 standard deviations above the mean (Fig. 5a), which coincided with the tropical IWV reservoir near

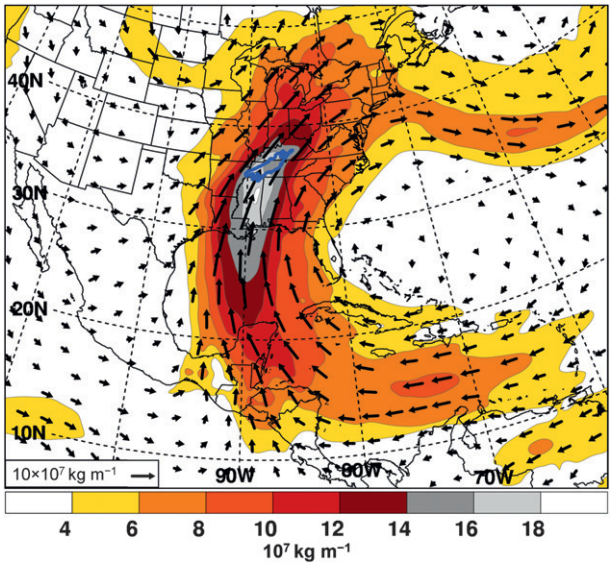

FIG. 7. 1000–300-hPa IVT (shaded in 10^6 kg m^{-1} with vectors overlaid; vector scale is shown at bottom left) integrated with respect to time from 0000 UTC 1 May to 0000 UTC 3 May 2010. The 200-mm rainfall contour for 0000 UTC 1 May–0000 UTC 3 May from the NPVU QPE product is shown in blue.

Central America (e.g., Fig. 4d). By 1200 UTC 2 May, this region of highly anomalous IWV appeared to have stretched poleward across the Yucatan Peninsula and the central Gulf of Mexico (Fig. 5b). Concurrently, IWV anomalies across the Gulf of Mexico and the south-central United States had increased to >2.5 standard deviations above the mean within a narrow band (Fig. 5b).

4. Physical processes supporting heavy rainfall

a. *Water vapor transport and AR formation*

1) VERTICALLY INTEGRATED WATER VAPOR FLUX

Following Neiman et al. (2008a), in order to quantify water vapor transport in an Eulerian framework and to verify the presence of an AR, vertically integrated water vapor fluxes [hereafter integrated vapor transport (IVT)] over North America are analyzed for 1–2 May. These fluxes were calculated as

$$-\int_{p_o}^{p} (q\mathbf{V})\frac{dp}{g}, \tag{1}$$

where q is the specific humidity, $\mathbf{V}$ is the horizontal wind, p_o is 1000 hPa, p is 300 hPa, and g is the acceleration due to gravity.

At 0000 UTC 1 May, a broad anticyclonically curved corridor of IVT values of 200–800 kg m^{-1} s^{-1} extended

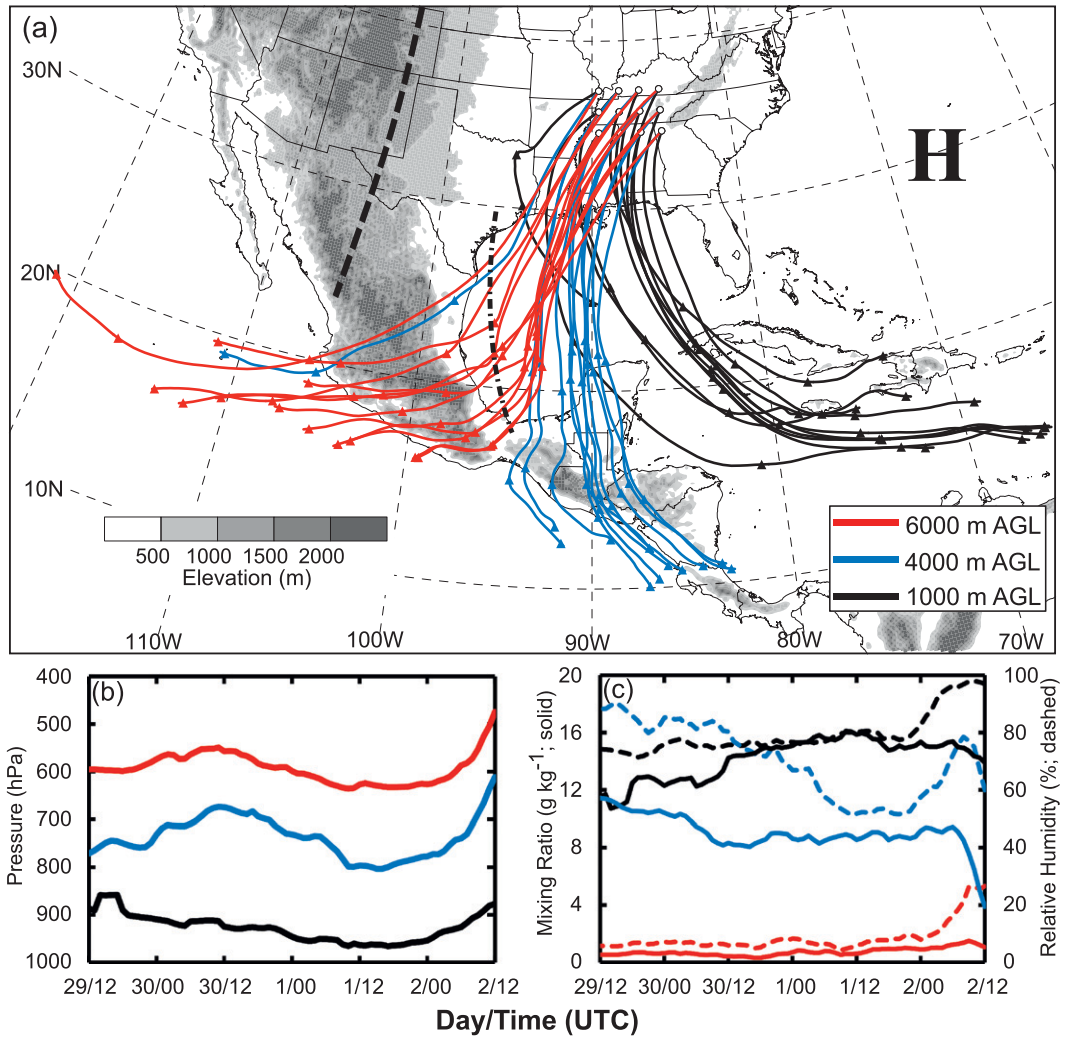

FIG. 8. (a) Three sets of twelve 72-h backward air parcel trajectories ending at 1200 UTC 2 May 2010 at 1000 m AGL (black), 4000 m AGL (blue), and 6000 m AGL (red) computed from the GDAS analyses using the HYSPLIT model. The triangles plotted along each trajectory mark the 1200 UTC air parcel positions, and the white circles denote the end point of each trajectory. Terrain elevation (m) is shaded according to the gray shaded bar. For reference, the position of the 850-hPa lee trough at 1200 UTC 2 May is denoted by the dashed–dotted line, and the position of the 850-hPa geopotential height maximum associated with the subtropical ridge at 1200 UTC 2 May is denoted by the "H" symbol. The position of the 250-hPa trough axis at 1200 UTC 2 May is marked by the thick dashed black line. (b) Time series of median hourly air pressure (hPa) along each set of trajectories [shaded as in (a)]. (c) Time series of median hourly MR (g kg^{-1}; solid lines) and median hourly RH (%; dashed lines) along each set of trajectories [shaded as in (a)]. Time series in (b) and (c) go from 1200 UTC 29 Apr (29/12) to 1200 UTC 2 May (2/12).

from the Caribbean Sea across the Gulf of Mexico and into the Great Lakes region (Fig. 6a). During 0000–1200 UTC 1 May, IVT intensified over the central Gulf of Mexico and the southern Mississippi Valley in the presence of enhanced confluence between southerly IVT extending across Central America, the Yucatan Peninsula, and the western Gulf of Mexico and southeasterly IVT extending across the Caribbean Sea and the eastern Gulf of Mexico (Figs. 6a,b). By 1200 UTC 1 May, a narrow band of IVT values of 800–1200 kg m^{-1} s^{-1} extended from the Louisiana coast into western Tennessee and Kentucky (Fig. 6b), intersecting the western flank of the first MCS (e.g., Fig. 1a). The narrow and concentrated distribution of IVT at 1200 UTC 1 May demonstrates the presence of an AR (see Neiman et al. 2008a, their Fig. 5).

During the subsequent 24-h period, the IVT corridor strengthened and became increasingly confluent across Central America, the Gulf of Mexico, and the southern Mississippi Valley (Figs. 6b–d). By 1200 UTC 2 May, the

IVT corridor had become exceptionally narrow and concentrated (Fig. 6d), with a 350-km-wide band of IVT values >800 kg m^{-1} s^{-1} extending from the Yucatan Peninsula to the central Great Lakes. At 1200 UTC 2 May, the core (values between 1200 and 1600 kg m^{-1} s^{-1}; maximum value of 1590 kg m^{-1} s^{-1}) of the IVT corridor extended from central Mississippi to southwestern Kentucky (Fig. 6d), intersecting the western flank of the second MCS (Fig. 1b). The maximum IVT value of 1590 kg m^{-1} s^{-1} at 1200 UTC 2 May is considerably larger than the maximum IVT values of ~1000 kg m^{-1} s^{-1} and ~650 kg m^{-1} s^{-1} found in recent case studies of strong landfalling ARs over the eastern North Pacific by Neiman et al. (2008b) and Ralph et al. (2011), respectively. This difference in IVT magnitude is likely attributable to the larger observed AR water vapor content for this event (maximum IWV value of 65 mm; Fig. 4h) compared with that observed for those two cases (maximum IWV values of ~50 and ~40 mm, respectively).

A factor that was likely fundamental regarding the long duration of heavy rainfall during 1–2 May 2010, resulting in extreme rainfall totals, was the marked persistence of intense IVT (Fig. 6) and anomalous IWV (Figs. 4 and 5) in the heavy rainfall region. This issue of persistence is demonstrated simply through a time integration of IVT from 0000 UTC 1 May to 0000 UTC 3 May, which yields a corridor of concentrated IVT directed across the Gulf of Mexico into the central Mississippi Valley (Fig. 7). Importantly, the region of heavy rainfall in Tennessee and Kentucky, represented in Fig. 7 by the 200-mm rainfall contour for 0000 UTC 1 May–0000 UTC 3 May, was positioned directly poleward of the core of the time-integrated IVT corridor.

2) TRAJECTORY ANALYSIS

To further investigate the transport of water vapor into the heavy rainfall region in Tennessee and Kentucky during 1–2 May 2010, we now assume a Lagrangian perspective through backward air parcel trajectory analysis. For this analysis, three groups of twelve 72-h backward air parcel trajectories ending at 1000 (~880), 4000 (~620), and 6000 m AGL (~500 hPa), respectively, within a 2.5° latitude × 5° longitude box centered over Tennessee were computed. For concision, we present only the results for trajectories ending at 1200 UTC 2 May (Fig. 8), an analysis time at which strong AR conditions were present (Fig. 6d). It should, however, be noted that qualitatively similar results were obtained when backward trajectories were computed for other times between 1200 UTC 1 May and 0000 UTC 3 May.

The trajectories demonstrate that winds veered with height over the Gulf of Mexico and the south-central United States, indicating geostrophic warm advection

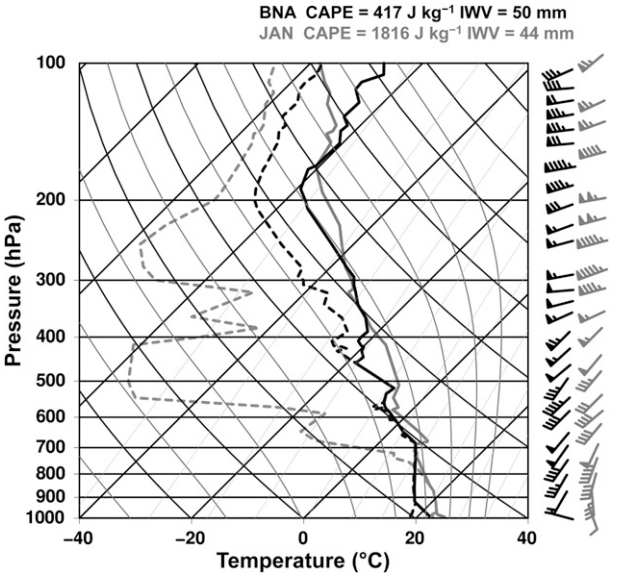

FIG. 9. Skew T–log$p$ plot showing temperature (°C; solid lines), dewpoint (°C; dashed lines), and wind (barbs in m s^{-1} according to the convention in Fig. 4) at 1200 UTC 1 May 2010 for BNA (black) and JAN (gray). CAPE and IWV values are provided at the top. The positions of BNA and JAN are marked in Fig. 10.

and corresponding to general ascending motion during 0000 UTC–1200 UTC 2 May (Figs. 8a,b). Air parcels ending at 1000 m AGL generally originated between the surface (~1015 hPa) and 2000 m AGL (~800 hPa; median pressure value of 890 hPa in Fig. 8b), within a relatively moist air mass [median relative humidity (RH) value of ~78% and median mixing ratio (MR) value of ~12 g kg^{-1}; Fig. 8c] over the Caribbean Sea (Fig. 8a). These parcels moistened (median MR value increasing to ~16 g kg^{-1}; Fig. 8c) along their trajectories, possibly in association with turbulent mixing in the marine PBL, and exhibited gradual descending motion (Fig. 8b) as they moved anticyclonically westward across the Caribbean Sea and into the Gulf of Mexico during 1200 UTC 29 April–1800 UTC 1 May. The air parcels subsequently moved poleward into the south-central United States (Fig. 8a) and gradually ascended between 1800 UTC 1 May and 1200 UTC 2 May. As the air parcels moved into the heavy rainfall region over Tennessee during 2 May, they exhibited increases in RH (median value increasing to ~98%) and decreases in water vapor content (median MR value decreasing to ~14 g kg^{-1}; Fig. 8c), suggesting that condensation and precipitation occurred along the trajectories.

Air parcels ending at 4000 m AGL generally originated between 800 m (~925 hPa) and 3000 m AGL (~700 hPa; median pressure value of 770 hPa in Fig. 8b) near Central America (Fig. 8a), a region which NOAA/NESDIS IWV imagery reveals was quite moist (IWV

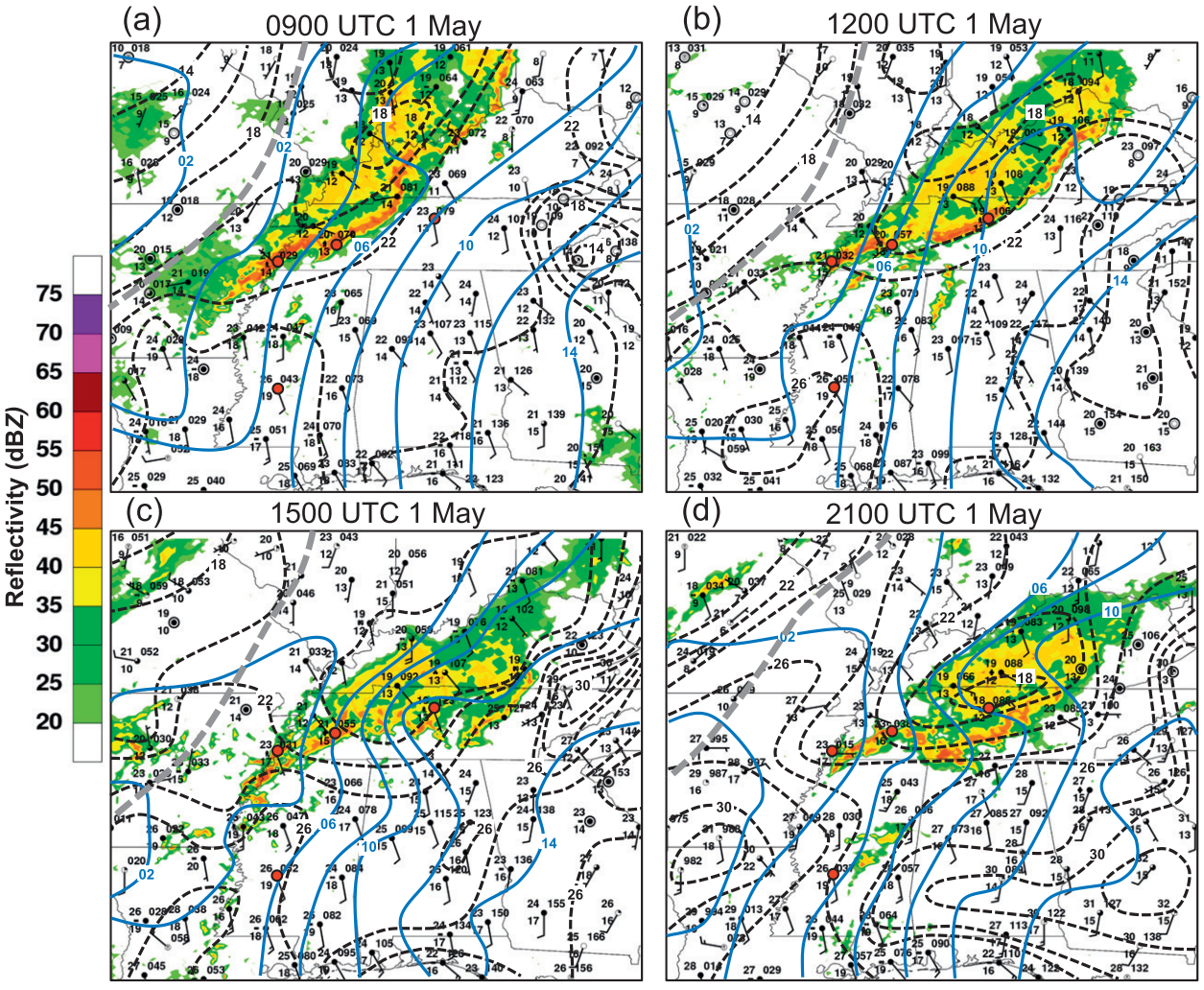

FIG. 10. Manual analysis of surface potential temperature (contoured in black every 2°C) and SLP (contoured in blue every 2 hPa) overlaid on WSR-88D base reflectivity imagery (shaded in dBZ according to the color bar) for (a) 0900 UTC 1 May, (b) 1200 UTC 1 May, (c) 1500 UTC 1 May, and (d) 2100 UTC 1 May 2010. The surface station models depict wind (barbs in m s^{-1} according to the convention in Fig. 4), potential temperature (°C; top-left quadrant of model), MR (g kg^{-1}; bottom-left quadrant of model), and SLP (hPa; top-right quadrant of model). The thick dashed gray line denotes the manually analyzed position of the surface cold front. The bold red dots mark the locations of, from south to north, JAN, MEM, MKL, and BNA.

values of 60–75 mm) during 29–30 April (not shown). Consequently, this set of air parcels began with relatively high RH and MR values (median values of ~90% and ~11 g kg^{-1}, respectively; Fig. 8c). As the parcels moved poleward and descended in the lee of the high terrain of Honduras, Guatemala, and southern Mexico during 1200 UTC 30 April–1200 UTC 1 May (Figs. 8a,b), the median parcel RH steadily decreased to ~50% and the median parcel MR stayed relatively constant at 8–10 g kg^{-1} (Fig. 8c), suggesting that the parcels warmed sensibly. Between 1200 UTC 1 May and 1200 UTC 2 May, the air parcels moved rapidly poleward across the central Gulf of Mexico and into the south-central United States (Fig. 8a), rapidly ascending (Fig. 8b) and losing large portions of their water vapor content (median MR value decreasing to ~4 g kg^{-1}; Fig. 8c) as they entered the heavy rainfall region between 0600 and 1200 UTC 2 May. This loss of water vapor content was likely associated with condensation and precipitation, but may also have been related to entrainment of dry midlevel air (note the drop in RH between 0600 and 1200 UTC 2 May; Fig. 8c).

Air parcels ending at 6000 m AGL originated between 4000 m (~640 hPa) and 5500 m AGL (~520 hPa; median pressure value of 595 hPa shown in Fig. 8b) within a very dry air mass (median RH value of ~6% and median MR value of ~0.5 g kg^{-1}; Fig. 8c) over the Pacific to the southwest of Mexico (Fig. 8a). These air

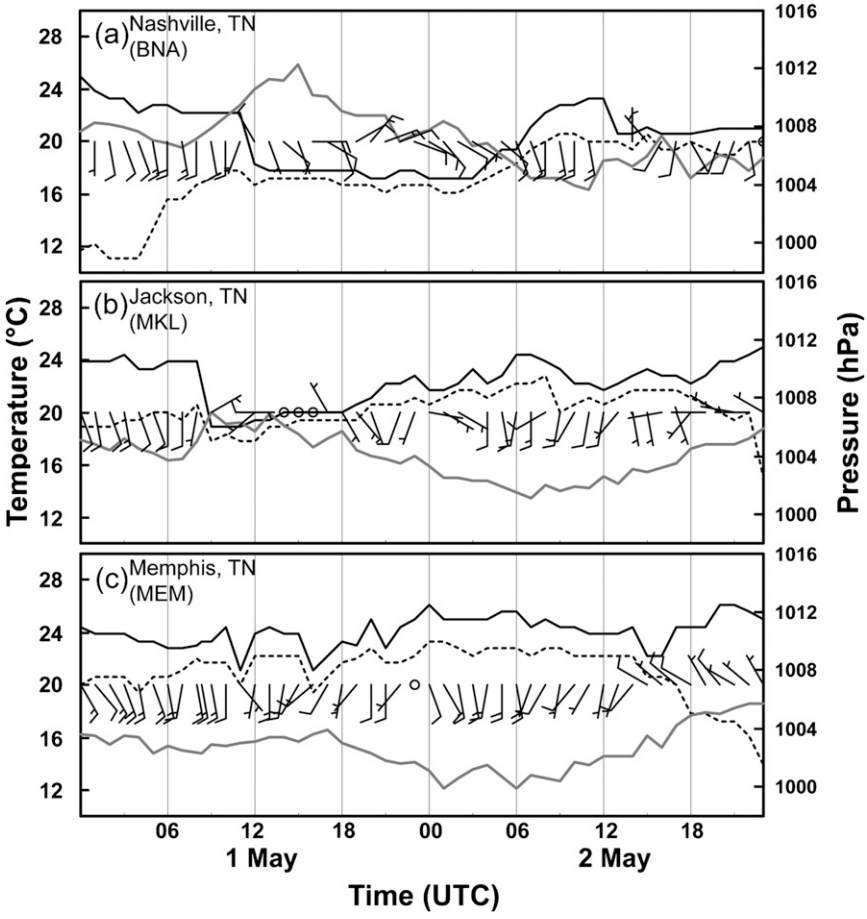

FIG. 11. Meteograms for 0000 UTC 1 May–0000 UTC 3 May 2010 of surface temperature (°C; solid black lines), surface dewpoint (°C; dashed black lines), SLP (hPa; gray lines), and surface wind (barbs in m s^{-1} according to the convention in Fig. 4) at (a) BNA, (b) MKL, and (c) MEM. The positions of BNA, MKL, and MEM are denoted in Fig. 10.

parcels generally remained quite dry (median RH values 5%–25% and median MR values of 0.5–1.5 g kg^{-1}; Fig. 8c) through the 72-h period as they moved cyclonically across the southern Mexican Plateau, the western Gulf of Mexico, and the south-central United States (Fig. 8a). During 0000–1200 UTC 2 May, the parcels accelerated northeastward downstream of the upper-level trough axis (Fig. 8a) and abruptly ascended, with median RH values remaining below 30% (Figs. 8b,c).

The trajectory analysis described above identifies two primary tropical source regions for moist air entering the heavy rainfall region in Tennessee and Kentucky: 1) over the Caribbean Sea (trajectories ending at 1000 m AGL), and 2) near Central America over the eastern tropical Pacific (trajectories ending at 4000 m AGL). Moving across the Caribbean Sea and the Gulf of Mexico at low levels, the air parcels ending at 1000 m AGL likely also acquired a portion of their water vapor content through turbulent mixing within the marine PBL. The confluence and superposition of the two moist airstreams over the central Gulf of Mexico along ~90°W during 1200 UTC 1 May–1200 UTC 2 May (Fig. 8a) appeared to approximately coincide with the formation of the plume of enhanced IWV (Figs. 3a–c and 4d,f,h) and with the intensification of the narrow corridor of IVT (i.e., the AR; Figs. 6b–d) across the Gulf of Mexico and the south-central United States. In general, air parcels entering the heavy rainfall region above ~600 hPa were exceptionally dry. The superposition of this dry midlevel air and the very moist air at lower levels likely provided a key mechanism for a buildup of CAPE, favoring deep moist convection and MCS development.

b. *Mesoscale analysis*

We have thus far shown that persistent heavy rainfall during 1–2 May 2010 across Tennessee and Kentucky, taking the form of two MCSs, was supported on the synoptic scale by strong water vapor transport from the

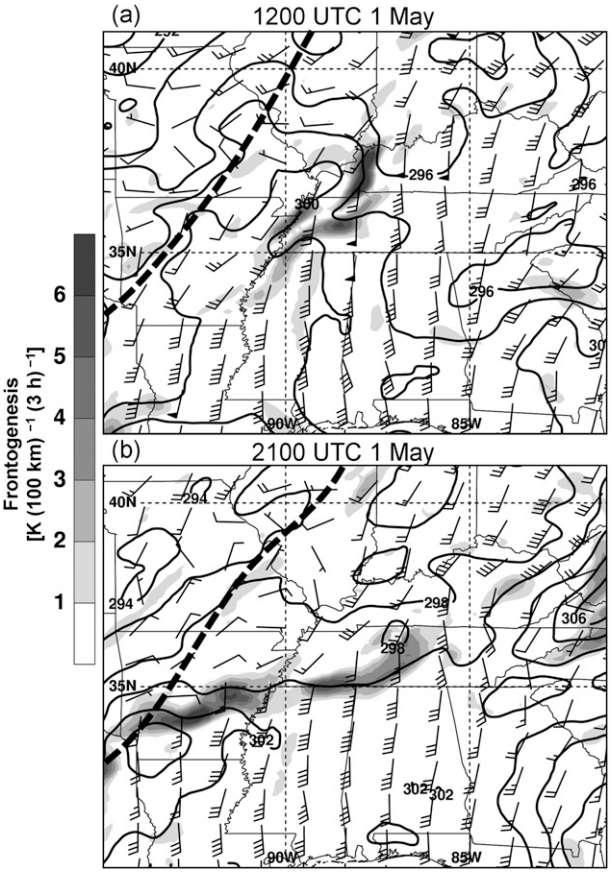

FIG. 12. 925-hPa potential temperature (contoured in black every 2°C), wind (barbs in m s^{-1} according to the convention in Fig. 4), and Petterssen frontogenesis [shaded in K $(100\ km)^{-1}$ $(3\ h)^{-1}$ according to the gray shaded bar] generated from the 13-km RUC analyses at (a) 1200 UTC 1 May and (b) 2100 UTC 1 May 2010. The manually analyzed position of the surface cold front is denoted by the thick dashed black line.

eastern tropical Pacific and the Caribbean Sea. In this section, we examine the mesoscale conditions and physical mechanisms associated with the continuous generation of deep moist convection.

1) FIRST PERIOD OF HEAVY RAINFALL: 1 MAY 2010

Soundings at 1200 UTC 1 May from Nashville, Tennessee (BNA), and Jackson, Mississippi (JAN) (Fig. 9), elucidate key characteristics of the environment that favored deep moist convection during the first period of heavy rainfall. At both BNA and JAN, very moist conditions were present, with observed IWV values of 50 and 44 mm, respectively. At BNA, which had a CAPE value of 417 J kg^{-1}, the environment was nearly saturated between the surface and 450 hPa, with two moist absolutely unstable layers (MAULs; Bryan and Fritsch 2000) evident between 700 and 575 hPa and between 525 and 450 hPa, respectively. Additionally, strong (20–30 m s^{-1}) southwesterly winds were present between 850 hPa and the tropopause, a wind profile favorable for the development of linearly organized MCSs (e.g., Parker and Johnson 2000). At JAN, a MAUL was evident from just above the surface to ~800 hPa, while very dry conditions and relatively steep lapse rates were in place aloft (note the elevated mixed layer between 700 and 600 hPa). This configuration in the JAN sounding was associated with a CAPE value of 1816 J kg^{-1} and was convectively unstable (i.e., equivalent potential temperature decreasing with increasing height; not shown). The low-level winds at JAN were strong and veered from south-southeasterly to southwesterly between the surface and 700 hPa, indicating the presence of low-level geostrophic warm advection, while strong (20–50 m s^{-1}) southwesterly winds prevailed aloft.

During 0900–1200 UTC 1 May, the first MCS, which was characterized by a ''trailing stratiform'' organizational mode (Parker and Johnson 2000), moved eastward across western Tennessee and western Kentucky ahead of the slow-moving synoptic-scale cold front extending southward from the cyclone over the northern plains (Figs. 10a,b). This eastward MCS movement occurred as the associated convectively generated cold pool progressed northeastward (Figs. 10a,b) in the direction of the southwesterly midlevel (i.e., ~700–400 hPa) flow (Fig. 9). With the arrival of the cold pool into Tennessee, abrupt temperature decreases and sea level pressure (SLP) increases were evident at Jackson, Tennessee (MKL), and BNA, while dewpoint temperatures remained consistently between 16° and 20°C at both locations (Figs. 11a,b).

As the cold pool pushed northeastward between 0900 and 1200 UTC, the trailing segment of the outflow boundary on its southwestern periphery, characterized by a surface potential temperature θ_{sfc} gradient of ~2 K $(100\ km)^{-1}$, became oriented parallel to the midlevel southwesterly flow and stalled along the southwestern Tennessee border (Figs. 10a,b). Intersected by moist (surface MR values of 15–19 g kg^{-1}) southerly surface flow and positioned in the vicinity of moderate CAPE (Fig. 9), this stationary segment of the outflow boundary became the focus for the repeated development of new convective (reflectivity values >45 dBZ) cells on the upstream (relative to the midlevel flow; Fig. 9) flank of the leading convective line (Figs. 10a,b), a process known as ''back building'' (e.g., Bluestein and Jain 1985; Schumacher and Johnson 2005). Surface convergence within the region of new cell development over southwestern Tennessee along the outflow boundary was evident during 0900–1200 UTC by a decrease in wind speed (~5 to 2.5 m s^{-1}) and a shift in wind direction (southerly to easterly) from Memphis, Tennessee (MEM),

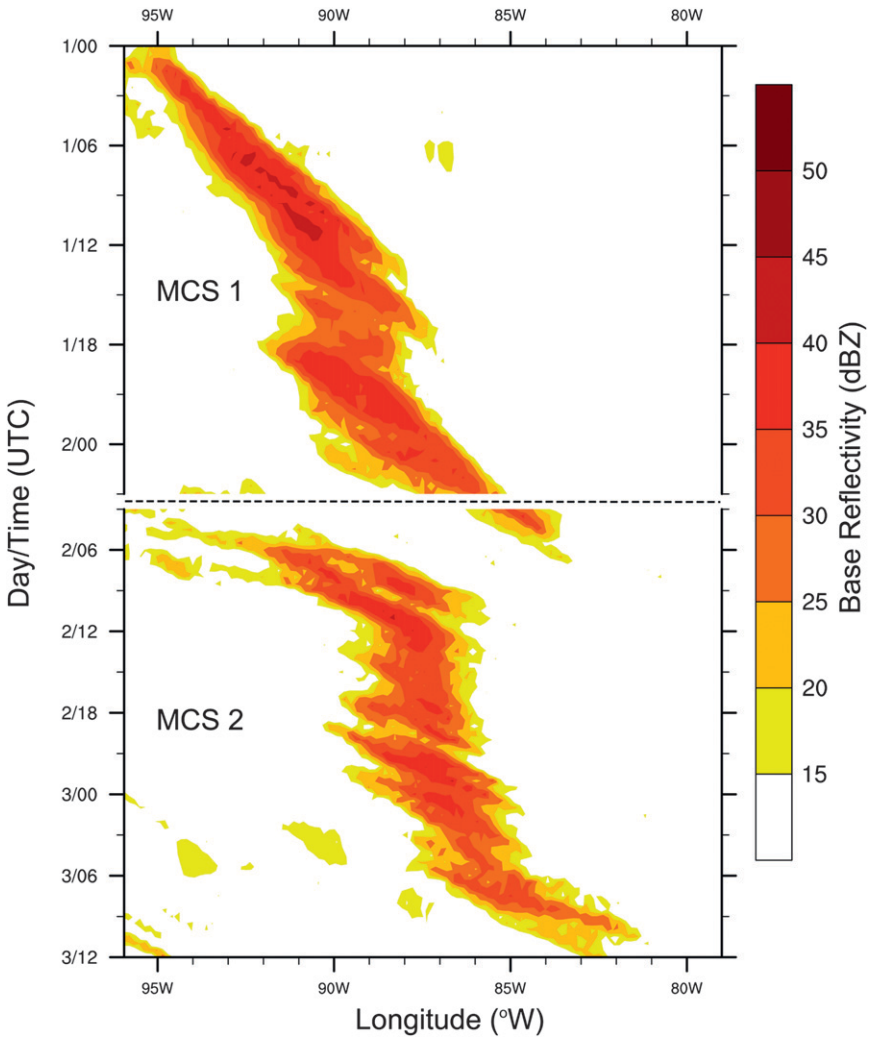

FIG. 13. Time–longitude plot of WSR-88D base reflectivity (shaded in dBZ according to the color bar) averaged between 33.5° and 35.0°N for 0000 UTC 1 May–0300 UTC 2 May 2010 (1/00–2/03) and between 35° and 36.5°N for 0300 UTC 2 May–1200 UTC 3 May 2010 (2/03–3/12).

to MKL (Figs. 11b,c). The convective line at 0900 and 1200 UTC appeared as a nearly contiguous band of reflectivity values of >45 dBZ (Figs. 10a,b), possibly indicating the presence of ''layer lifting'' along the outflow boundary (James et al. 2005). Layer lifting, consistent with the observed MAULs at 1200 UTC at BNA and JAN (Fig. 9; Bryan and Fritsch 2000), was plausibly forced in connection with the interaction of the southerly LLJ with the outflow boundary (e.g., James et al. 2005), a signature of which was a band of strong 925-hPa frontogenesis[2] over western Tennessee at 1200 UTC (Fig. 12a).

During 1200–2100 UTC 1 May, concurrent with the development of a mesoscale SLP ridge, or ''mesohigh'' (e.g., Maddox et al. 1979), over central Tennessee and Kentucky, the cold pool was enhanced (Figs. 10b–d), likely in connection with evaporational cooling across Tennessee and Kentucky. Concurrently, the stationary outflow boundary over southwestern Tennessee strengthened, with its associated θ_{sfc} gradient increasing to ~7 K (100 km)$^{-1}$ by 2100 UTC (Fig. 10d). During this time period, winds to the north of the outflow boundary at BNA and MKL became increasingly easterly while winds just to the south over northern Mississippi and Alabama remained southerly (Figs. 10b–d and 11a,b). Between 1500 and 2100 UTC, the organizational mode of the MCS came to resemble the training line/adjoining stratiform (TL/AS) extreme-rain-producing

[2] Frontogenesis calculations in the present study were done using the Petterssen frontogenesis equation (Petterssen 1936, 1956, 200–201), following the method of Keyser et al. [1988; their Eqs. (1.1)–(1.4)].

MCS archetype documented by Schumacher and Johnson (2005), with new convective cells continuously developing on the upstream flank of the convective line (i.e., back building) while older cells moved down stream across central Tennessee approximately parallel to the convective line, a process commonly called ''echo training,'' and eventually dissipated (Figs. 10c,d). By the 2100 UTC, the MCS was positioned parallel to and on the cool side of the outflow boundary (Fig. 10d) in the vicinity of strong 925-hPa frontogenesis established at the intersection of the LLJ with the outflow boundary (Fig. 12b).

The back building of convection observed between 0900 and 2100 UTC 1 May yielded an MCS that was nearly stationary during the time period. This situation is depicted clearly by a time–longitude plot of radar reflectivity (Fig. 13), with data averaged between 33.5° and 35.0°N for 0000 UTC 1 May–0300 UTC 2 May and between 35° and 36.5°N for 0300 UTC 2 May–1200 UTC 3 May. This plot shows the initial eastward progression of the first MCS between 0000 and 0900 UTC 1 May followed by a conspicuous stalling of the MCS during 0900–2100 UTC between ~91° and ~88°W, reflecting the back-building process. The MCS eventually progressed eastward while dissipating after 0000 UTC 2 May.

2) SECOND PERIOD OF HEAVY RAINFALL: 2 MAY 2010

Soundings from BNA and JAN at 1200 UTC 2 May (Fig. 14) depict favorable environmental conditions for deep moist convection during the second period of heavy rainfall. The conditions at BNA and JAN were characterized by large water vapor content (IWV values of 50 and 47 mm, respectively) and moderate CAPE (values of 1227 and 1766 J kg^{-1}, respectively). At both locations very moist conditions in the lowest 300 hPa were topped by dry conditionally unstable layers aloft (~700–480 hPa at BNA; ~850–650 and ~550–350 hPa at JAN), consistent with the moderate CAPE values and corresponding to convective instability (not shown). Importantly, at both locations weak convective inhibition was evident, indicating that only weak lifting was required for CAPE to be released. At BNA, the dry conditionally unstable layer was capped by a conspicuous layer of strong static stability and substantial moistening with height between ~470 and ~400 hPa, indicative of the presence of an upper-level frontal zone and consistent with the smaller observed CAPE at BNA compared with JAN. Winds at BNA and JAN veered from southerly to southwesterly with height in the lowest 300 hPa, indicating the presence of low-level geostrophic warm advection, while strong (25–45 m s^{-1}) southwesterly flow prevailed above 700 hPa at both locations.

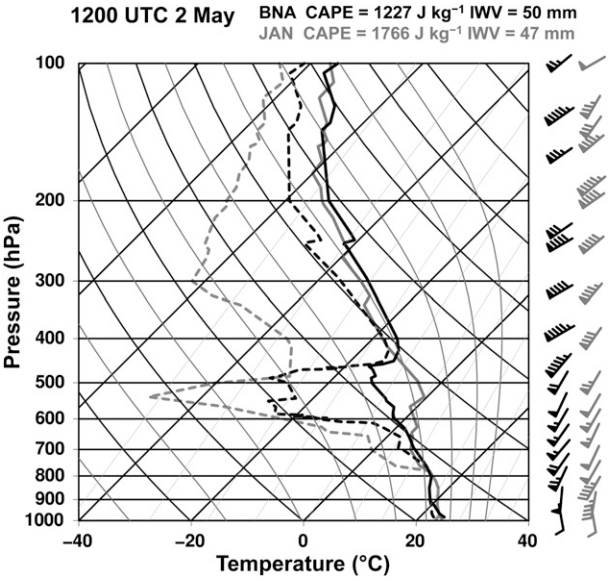

FIG. 14. As in Fig. 9, but for 1200 UTC 2 May 2010.

Between 0000 and 0900 UTC 2 May (not shown), widespread convection developed across western portions of Tennessee and Kentucky along the remnant outflow boundary associated with the first MCS. This convection appeared to be initiated in conjunction with the passage of the previously discussed low-level mesoscale frontal wave, which was represented at 0900 UTC by an SLP trough (labeled ''L'' in Fig. 15a) over northeastern Arkansas, southeastern Missouri, and southern Illinois. During 0900–1500 UTC, convection became linearly organized, resembling the parallel stratiform (PS) MCS archetype documented by Parker and Johnson (2000), and stretched from northern Mississippi to central Kentucky on the warm side (i.e., to the east) of the slow-moving synoptic-scale cold front associated with the northern plains cyclone (Figs. 15a–c). This mesoscale organization took shape as individual convective cells and adjoining regions of stratiform precipitation moved rapidly northeastward (Figs. 15a–c) in the direction of the strong midlevel (i.e., ~800–450 hPa) southwesterly flow (Fig. 13), a key process in the formation of PS MCSs (Parker and Johnson 2000; Parker 2007). Individual convective cells associated with the MCS generally moved parallel to the convective line, repeatedly training through a narrow corridor across northern Mississippi, west-central Tennessee, including the Nashville area, and central Kentucky (Figs. 15a–c).

During 1200–1500 UTC, the acquisition of the linear structure of the MCS was concurrent with the formation of an elongated surface cold pool parallel to the axis of convection (Figs. 15b,c). The formation of the cold pool

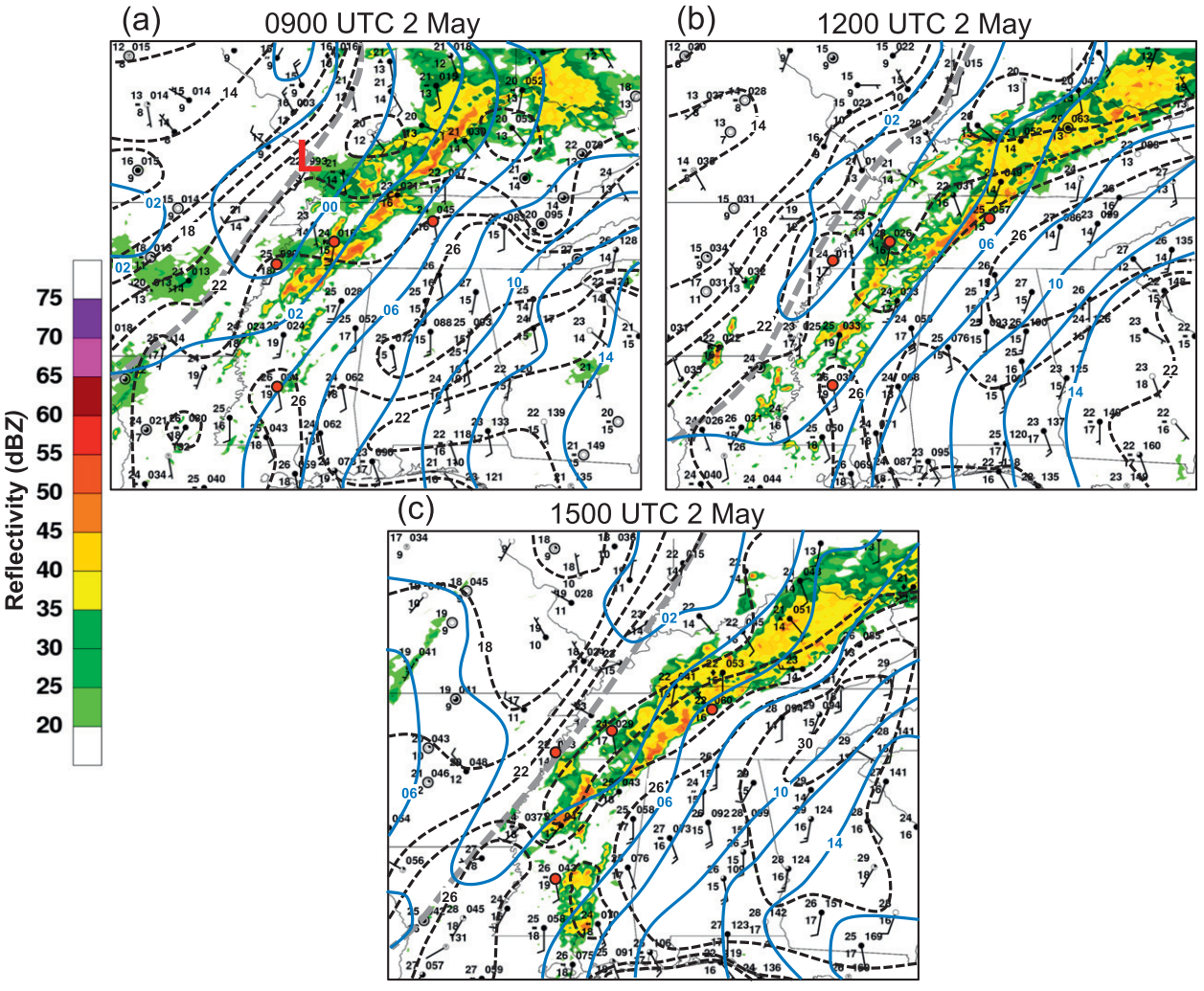

FIG. 15. As in Fig. 10, but for (a) 0900 UTC 2 May, (b) 1200 UTC 2 May, and (c) 1500 UTC 2 May 2010. The "L" symbol in (a) marks the position of the SLP minimum associated with the frontal wave described in the text.

was marked by a relatively modest temperature decrease of 3°C at BNA, whereas at MKL and MEM significant temperature changes were nearly absent (Fig. 11), owing to the relatively narrow structure of the cold pool (Figs. 15b,c). The outflow boundary on the southern periphery of the cold pool, with a θ_{sfc} gradient of ~3.5 K $(100\ km)^{-1}$, was oriented parallel to the southwesterly midlevel flow and was nearly stationary (Fig. 15b,c). The MCS exhibited back building during 1200–1500 UTC as new convective cells developed on the southwestern flank of the convective line along of the outflow boundary in the presence of moist (MR values of 16–18 g kg^{-1}) southerly surface flow (Figs. 15b,c). This back building of convection coincided with the development of 925-hPa frontogenesis over northern Mississippi, central Tennessee, and central Kentucky at the intersection of the southerly LLJ with the outflow boundary (Figs. 16a,b).

The repeated development of new convective cells approximately balanced the northeastward motion of older convective cells and thereby caused the second MCS to be nearly stationary during its life span (Figs. 15b,c; e.g., Chappell 1986; Corfidi 2003). This stationary nature of the second MCS is demonstrated in Fig. 13 by a stationary column of reflectivity values of 15–40 dBZ confined between ~88° and ~86°W during ~0900 UTC 2 May–0000 UTC 3 May. In addition, this column was traversed by eastward-moving streaks of enhanced reflectivity, representing the training of individual convective cells within the stationary convective line.

5. Synthesis and conclusions

Two consecutive periods of heavy rainfall during 1–2 May 2010 associated with two successive quasi-stationary

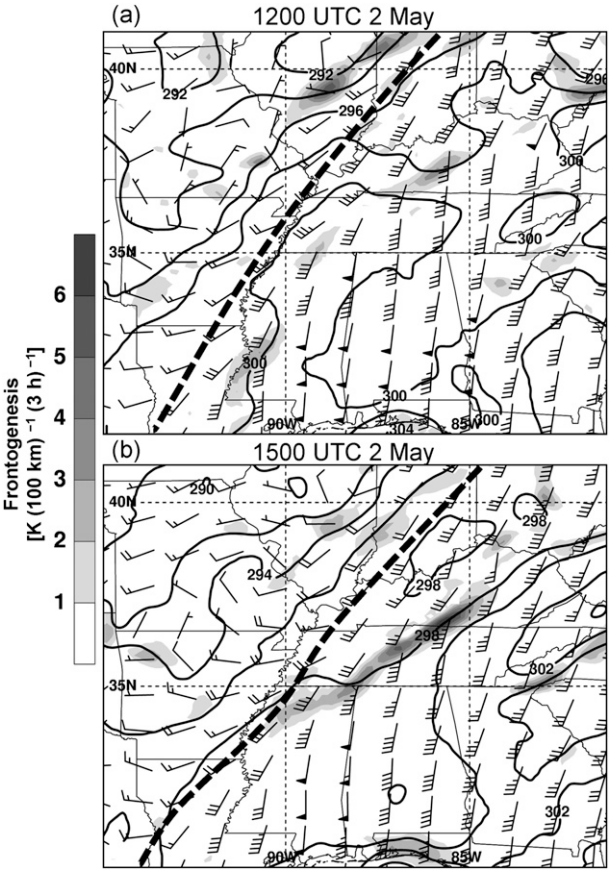

FIG. 16. As in Fig. 12, but for (a) 1200 UTC 2 May and (b) 1500 UTC 2 May 2010.

MCSs resulted in record-breaking rainfall totals and devastating flooding across portions of Tennessee and Kentucky, including the Nashville area. In the present study, a multiscale examination of the physical processes associated with this high-impact event was conducted. The key results are discussed in the text below and illustrated schematically in Fig. 17.

A primary finding of the present study was that heavy rainfall associated with MCS development during 1–2 May was supported by a persistent narrow corridor of strong water vapor transport (thick blue arrow in Fig. 17) rooted over the eastern tropical Pacific and the Caribbean Sea that was manifested as an AR (e.g., Newell et al. 1992; Zhu and Newell 1998; Ralph et al. 2004). Results indicate that, in contrast to oft-documented maritime ARs, which are migratory features that develop over ocean basins in connection with the precold-frontal LLJ associated with extratropical cyclones, the AR discussed in the present study was a static feature, developing in association with stationary synoptic-scale flow features (i.e., the lee trough along the eastern coast of Mexico and the subtropical ridge) that maintained strong and persistent confluent poleward low-level flow (i.e., the LLJ) from the tropics across the Gulf of Mexico and the south-central United States (Fig. 17). The persistence of the poleward flow allowed tropical water vapor to be continuously ''tapped'' and transported poleward into the heavy rainfall region, analogous to the ''tropical tap'' process discussed by Ralph et al. (2011) in the context of an AR event over the eastern North Pacific.

Akin to the precipitation impacts commonly associated with landfalling maritime ARs (e.g., Ralph et al. 2006; Neiman et al. 2008a,b, 2011; Stohl et al. 2008), the AR in the present study contributed to the generation of persistent heavy rainfall, which was anchored over Tennessee and Kentucky during 1–2 May 2010. However, the mesoscale processes by which heavy rainfall was generated and anchored during the May 2010 event were fundamentally distinct from those typically associated with landfalling maritime ARs, occurring in connection with two quasi-stationary MCSs as opposed to persistent orographically forced stratiform/shallow convective precipitation. For each MCS, new convective cells repeatedly developed on the upstream flank of the convective line (i.e., back building) while older cells moved downstream parallel to the convective line (i.e., echo training). In this scenario, the vector sum of the propagation and advection components of the system motion (e.g., Chappell 1986; Doswell et al. 1996; Corfidi 2003) was nearly zero for each MCS, causing each MCS to be quasi-stationary and resulting in prolonged heavy rainfall across Tennessee and Kentucky during 1–2 May.

The synoptic-scale configuration within which the two MCSs developed (Fig. 17) closely resembled the classic ''synoptic'' type flash-flood pattern documented by Maddox et al. (1979), with MCS development occurring 1) downstream of a high-amplitude, slow-moving upper-level trough, 2) on the warm side of a slow-moving synoptic-scale cold front, and 3) in the presence of a warm, moist, and unstable airstream (i.e., the AR) transported by strong low-level winds (i.e., the LLJ). The AR extending into the central Mississippi Valley on the warm side of the slow-moving cold front remained generally stationary during 1–2 May, affording a continuous supply of abundant water vapor and, overlaid by a midlevel stream of dry and conditionally unstable air, moderate CAPE. On the mesoscale, lifting necessary to continuously realize CAPE and to ''rain out'' the water vapor supply over Tennessee and Kentucky was forced in connection with low-level convergence and frontogenesis at the intersection of the LLJ with quasi-stationary convectively generated outflow boundaries (thin dashed black lines in Fig. 17) oriented approximately parallel to the ambient midlevel flow. This mesoscale scenario resembles the mesohigh-type flash-flood pattern

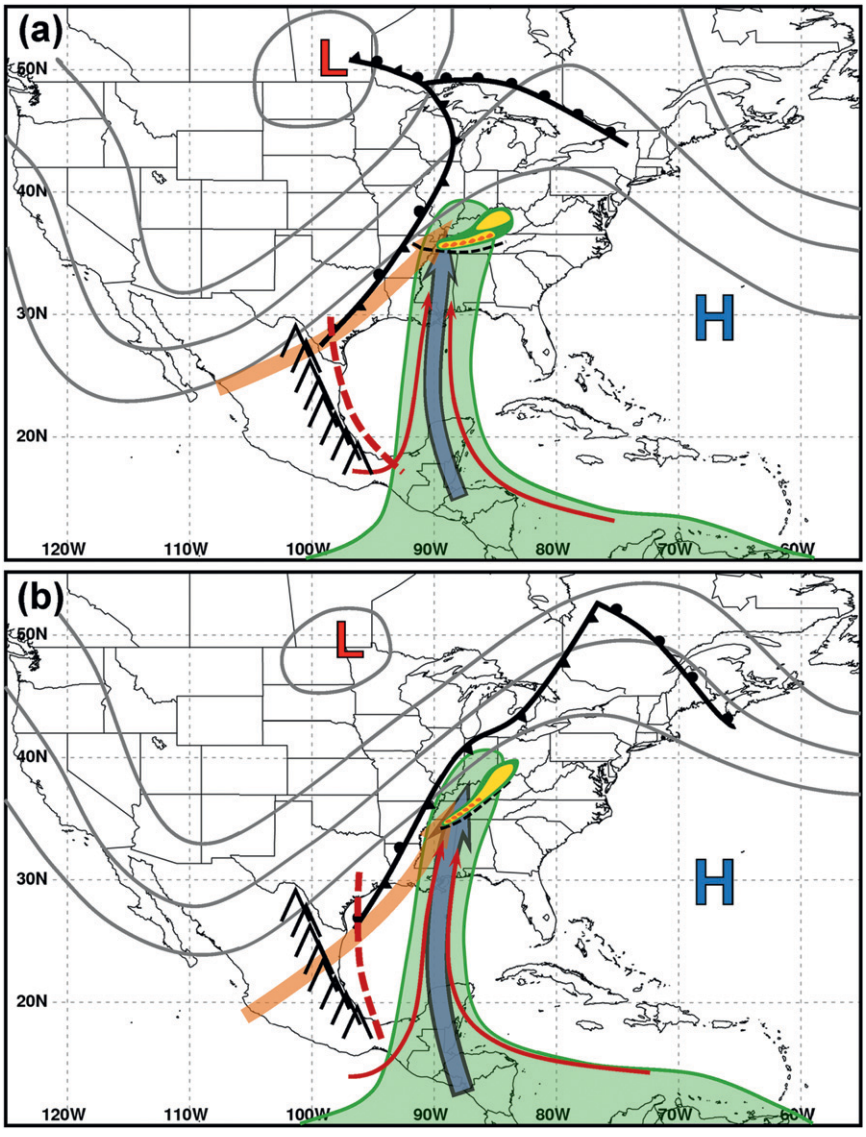

FIG. 17. Schematic illustrations of the key features and processes for (a) the 1 May MCS and (b) the 2 May MCS. The gray contours denote the 250-hPa geopotential height distribution. The red arrows represent 850-hPa streamlines. The positions of the surface fronts are shown in standard frontal notation, while the positions of the maxima and minima in 850-hPa geopotential height are marked by the "H" and the "L" symbols, respectively. The axis of the 850-hPa lee trough is denoted by the dashed red line. The light green shading outlines the regions with IWV values >45 mm. The thick orange arrows represent the stream of dry midlevel air, while the thick blue arrows represent the AR. The "∧" symbols mark the location of the Sierra Madre Oriental Mountains. The dashed black lines mark the positions of the convectively generated outflow boundaries, and the dark green, gold, and orange shaded regions over TN and KY represent radar reflectivity thresholds of 20, 35, and 50 dB*Z*, respectively.

of Maddox et al. (1979) and has been similarly documented in numerous studies of quasi-stationary MCSs (e.g., Bosart and Sanders 1981; Chappell 1986; Corfidi 2003; Schumacher and Johnson 2005; Ducrocq et al. 2008).

In summary, a number of synoptic- and mesoscale ingredients, common in environments associated with heavy rainfall events and flash floods, came together to produce extreme flooding rainfall across Tennessee and Kentucky during 1–2 May 2010 and included 1)

persistent strong IVT and anomalous IWV associated with a stationary AR, 2) persistent mesoscale lifting associated with quasi-stationary convectively generated outflow boundaries, and 3) MCS organization featuring back building and echo training. The extreme, unprecedented (>1000-yr recurrence interval) rainfall observed during this event, which distinguishes it from ''typical'' heavy rainfall events, likely resulted from the combined *persistence* of these ingredients over the same region during 1–2 May. Further analysis would be required to quantitatively test this hypothesis.

The results of the present study point to several avenues for future research. We have documented the meteorological conditions and physical processes associated with an AR extending into the central United States; however, because the results stem from just a single case, it is unclear how applicable they may be to other AR-related events in the central United States. In this regard, future studies could possibly examine 1) the climatological characteristics, 2) the common environmental conditions, and 3) the production of heavy precipitation associated with central U.S. AR events. Additionally, a comprehensive assessment of the predictability of this and other similar events by numerical models would likely provide operational forecasters with valuable information and guidance when faced with possible high-impact heavy rainfall/flooding situations in the central United States.

Acknowledgments. The authors thank Bob Zamora (NOAA/ESRL), Dr. John Brown (NOAA/ESRL), Dr. Thomas Galarneau (NCAR), Dr. Kelly Mahoney (NOAA/ESRL), Ellen Sukovich (CIRES/NOAA/ESRL), and Michael Bodner (HPC) for their helpful comments and suggestions regarding this research. The authors also thank Dr. Russ Schumacher (Colorado State University) and two anonymous reviewers for their thoughtful comments, which greatly improved the quality of this manuscript. Dr. Jason Cordeira (NOAA/ESRL) is acknowledged for providing the NCEP–NCAR reanalysis climatological data and the base reflectivity mosaics and for his general technical assistance. Sheldon Kusselson (NOAA/NESDIS) provided the NOAA/NESDIS blended satellite IWV imagery. The MIMIC IWV imagery in the electronic supplement was provided by CIMSS at the University of Wisconsin—Madison. This research was supported by NOAA's Hydrometeorological Testbed.

REFERENCES

Augustine, J. A., and K. W. Howard, 1991: Mesoscale convective complexes over the United States during 1986 and 1987. *Mon. Wea. Rev.,* **119,** 1575–1589.

Bao, J.-W., S. A. Michelson, P. J. Neiman, F. M. Ralph, and J. M. Wilczak, 2006: Interpretation of enhanced integrated water vapor bands associated with extratropical cyclones: Their formation and connection to tropical moisture. *Mon. Wea. Rev.,* **134,** 1063–1080.

Bell, G. D., and J. E. Janowiak, 1995: Atmospheric circulation associated with the Midwest floods of 1993. *Bull. Amer. Meteor. Soc.,* **76,** 681–696.

Benjamin, S. G., and Coauthors, 2004: An hourly assimilation-forecast cycle: The RUC. *Mon. Wea. Rev.,* **132,** 495–518.

Benton, G. S., and M. A. Estoque, 1954: Water-vapor transfer over the North American continent. *J. Meteor.,* **11,** 462–477.

Bluestein, H. B., and M. H. Jain, 1985: Formation of mesoscale lines of precipitation: Severe squall lines in Oklahoma during the spring. *J. Atmos. Sci.,* **42,** 1711–1732.

Bosart, L. F., and F. H. Carr, 1978: A case study of excessive rainfall centered around Wellsville, New York, 20–21 June 1972. *Mon. Wea. Rev.,* **106,** 348–362.

——, and F. Sanders, 1981: The Johnstown flood of July 1977: A long-lived convective system. *J. Atmos. Sci.,* **38,** 1616–1642.

Browning, K. A., 1990: Organization of clouds and precipitation in extratropical cyclones. *Extratropical Cyclones: The Erik Palmén Memorial Volume,* C. W. Newton and E. Holopainen, Eds., Amer. Meteor. Soc., 129–153.

Bryan, G. H., and J. M. Fritsch, 2000: Moist absolute instability: The sixth static stability state. *Bull. Amer. Meteor. Soc.,* **81,** 1207–1230.

Carlson, T. N., 1991: *Mid-Latitude Weather Systems*. Harper-Collins, 507 pp.

Chappell, C. F., 1986: Quasi-stationary convective events. *Mesoscale Meteorology and Forecasting,* P. S. Ray, Ed., Amer. Meteor. Soc., 289–309.

Corfidi, S. F., 2003: Cold pools and MCS propagation: Forecasting the motion of downwind- developing MCSs. *Wea. Forecasting,* **18,** 997–1017.

Dettinger, M. D., 2004. Fifty-two years of ''pineapple-express'' storms across the west coast of North America. PIER project Rep. CEC-500-2005-004, U.S. Geological Survey, Scripps Institution of Oceanography for the California Energy Commission, PIER Energy-Related Environmental Research, 15 pp. [Available online at http://www.energy.ca.gov/2005publications/CEC-500-2005-004/CEC-500-2005-004.PDF.]

——, F. M. Ralph, T. Das, P. J. Neiman, and D. Cayan, 2011: Atmospheric rivers, floods, and the water resources of California. *Water,* **3,** 455–478.

Dirmeyer, P. A., and J. L. Kinter III, 2009: The Maya Express—Late spring floods in the US Midwest. *Eos, Trans. Amer. Geophys. Union,* **90,** 101–102.

——, and ——, 2010: Floods over the U.S. Midwest: A regional water cycle perspective. *J. Hydrometeor.,* **11,** 1172–1181.

Djurić, D., and M. S. Damiani, 1980: On the formation of the low-level jet over Texas. *Mon. Wea. Rev.,* **108,** 1854–1865.

Doswell, C. A., III, H. E. Brooks, and R. A. Maddox, 1996: Flash flood forecasting: An ingredients-based methodology. *Wea. Forecasting,* **11,** 560–581.

Draxler, R. R., and G. D. Hess, 1997: Description of the HYSPLIT_4 modeling system. NOAA Tech. Memo. ERL ARL-224, NOAA/Air Resources Laboratory, Silver Spring, MD, 24 pp.

——, and G. D. Rolph, cited 2011: HYSPLIT (HYbrid Single-Particle Lagrangian Integrated Trajectory) model. NOAA/Air Resources Laboratory, Silver Spring, MD. [Available online at http://ready.arl.noaa.gov/HYSPLIT.php.]

Ducrocq, V., O. Nuissier, D. Ricard, C. Lebeaupin, and T. Thouvenin, 2008: A numerical study of three catastrophic precipitating events over southern France. Part II: Mesoscale triggering and stationarity factors. *Quart. J. Roy. Meteor. Soc.,* **134,** 131–145.

Galarneau, T. J., Jr., L. F. Bosart, and R. S. Schumacher, 2010: Predecessor rain events ahead of tropical cyclones. *Mon. Wea. Rev.,* **138,** 3272–3297.

Halverson, J. B., and T. D. Rabenhorst, 2010: Mega-snow in the Megalopolis: The Mid-Atlantic's blockbuster winter of 2009–2010. *Weatherwise,* **63,** 16–23.

Hart, R. E., and R. H. Grumm, 2001: Using normalized climatological anomalies to rank synoptic-scale events objectively. *Mon. Wea. Rev.,* **129,** 2426–2442.

Higgins, R. W., Y. Yao, E. S. Yarosh, J. E. Janowiak, and K. C. Mo, 1997: Influence of the Great Plains low-level jet on summertime precipitation and moisture transport over the central United States. *J. Climate,* **10,** 481–507.

——, W. Shi, and C. Hain, 2004: Relationships between Gulf of California moisture surges and precipitation in the southwestern United States. *J. Climate,* **17,** 2983–2997.

——, V. E. Kousky, and P. Xie, 2011: Extreme precipitation events in the south-central United States during May and June 2010: Historical perspective, role of ENSO, and trends. *J. Hydrometeor.,* **12,** 1056–1070.

Hobbs, P. V., J. D. Locatelli, and J. E. Martin, 1996: A new conceptual model for cyclones generated in the lee of the Rocky Mountains. *Bull. Amer. Meteor. Soc.,* **77,** 1169–1178.

Hoskins, B., I. Draghici, and H. Davies, 1978: A new look at the ω-equation. *Quart. J. Roy. Meteor. Soc.,* **104,** 31–38.

James, R. P., J. M. Fritsch, and P. M. Markowski, 2005: Environmental distinctions between cellular and slabular convective lines. *Mon. Wea. Rev.,* **133,** 2669–2691.

Junker, N. W., R. S. Schneider, and S. L. Fauver, 1999: A study of heavy rainfall events during the Great Midwest Flood of 1993. *Wea. Forecasting,* **14,** 701–712.

Kalnay, E., and Coauthors, 1996: The NCEP/NCAR 40-Year Reanalysis Project. *Bull. Amer. Meteor. Soc.,* **77,** 437–472.

Keyser, D., M. J. Reeder, and R. J. Reed, 1988: A generalization of Petterssen's frontogenesis function and its relation to the forcing of vertical motion. *Mon. Wea. Rev.,* **116,** 762–780.

Kidder, S. Q., and A. S. Jones, 2007: A blended satellite total precipitable water product for operational forecasting. *J. Atmos. Oceanic Technol.,* **24,** 74–81.

Knippertz, P., and J. E. Martin, 2005: Tropical plumes and extreme precipitation in subtropical and tropical West Africa. *Quart. J. Roy. Meteor. Soc.,* **131,** 2337–2365.

——, and ——, 2007: A Pacific moisture conveyor belt and its relationship to a significant precipitation event in the semiarid southwestern United States. *Wea. Forecasting,* **22,** 125–144.

——, and H. Wernli, 2010: A Lagrangian climatology of tropical moisture exports to the Northern Hemispheric extratropics. *J. Climate,* **23,** 987–1003.

Lackmann, G. M., and J. R. Gyakum, 1999: Heavy cold-season precipitation in the northwestern United States: Synoptic climatology and an analysis of the flood of 17–18 January 1986. *Wea. Forecasting,* **14,** 687–700.

Maddox, R. A., C. F. Chappell, and L. R. Hoxit, 1979: Synoptic and meso-α scale aspects of flash flood events. *Bull. Amer. Meteor. Soc.,* **60,** 115–123.

Martin, J. E., J. D. Locatelli, P. V. Hobbs, P.-Y. Wang, and J. A. Castle, 1995: Structure and evolution of winter cyclones in the central United States and their effects on the distribution of precipitation. Part I: A synoptic-scale rainband associated with a dryline and lee trough. *Mon. Wea. Rev.,* **123,** 241–264.

McDonald, B. E., and M. N. Baker, 2001: The NWS National QPF Verification Program. COMET RFC/HPC Hydrometeorology course 02-1. [Available online at http://www.hpc.ncep.noaa.gov/npvu/confpres/hydromet02/hydromet02_1.pdf.]

Mo, K. C., J. Nogues-Paegle, and J. Paegle, 1995: Physical mechanisms of the 1993 summer floods. *J. Atmos. Sci.,* **52,** 879–895.

Moore, J. T., F. H. Glass, C. E. Graves, S. M. Rochette, and M. J. Singer, 2003: The environment of warm-season elevated thunderstorms associated with heavy rainfall over the central United States. *Wea. Forecasting,* **18,** 861–878.

National Weather Service, 2011: Record floods of Greater Nashville: Including flooding in middle Tennessee and western Kentucky, May 1–4, 2010. NWS Service Assessment, 93 pp. [Available online at http://www.weather.gov/os/assessments/pdfs/Tenn_Flooding.pdf.]

Neiman, P. J., F. M. Ralph, G. A. Wick, J. Lundquist, and M. D. Dettinger, 2008a: Meteorological characteristics and overland precipitation impacts of atmospheric rivers affecting the West Coast of North America based on eight years of SSM/I satellite observations. *J. Hydrometeor.,* **9,** 22–47.

——, ——, ——, Y.-H. Kuo, T.-K. Wee, Z. Ma, G. H. Taylor, and M. D. Dettinger, 2008b: Diagnosis of an intense atmospheric river impacting the Pacific Northwest: Storm summary and offshore vertical structure observed with COSMIC satellite retrievals. *Mon. Wea. Rev.,* **136,** 4398–4420.

——, L. J. Schick, F. M. Ralph, M. Hughes, and G. A. Wick, 2011: Flooding in western Washington: The connection to atmospheric rivers. *J. Hydrometeor.,* **12,** 1337–1358.

Newell, R. E., N. E. Newell, Y. Zhu, and C. Scott, 1992: Tropospheric rivers?—A pilot study. *Geophys. Res. Lett.,* **19,** 2401–2404.

Parker, M. D., 2007: Simulated convective lines with parallel stratiform precipitation. Part I: An archetype for convection in along-line shear. *J. Atmos. Sci.,* **64,** 267–288.

——, and R. H. Johnson, 2000: Organizational modes of midlatitude mesoscale convective systems. *Mon. Wea. Rev.,* **128,** 3413–3436.

Petterssen, S., 1936: Contribution to the theory of frontogenesis. *Geofys. Publ.,* **11** (6), 1–27.

——, 1956: *Motion and Motion Systems*. Vol. 2, *Weather Analysis and Forecasting,* McGraw-Hill, 428 pp.

Ralph, F. M., and M. D. Dettinger, 2011: Storms, floods, and the science of atmospheric rivers. *Eos, Trans. Amer. Geophys. Union,* **92,** 265–266.

——, P. J. Neiman, D. E. Kingsmill, P. O. G. Persson, A. B. White, E. T. Strem, E. D. Andrews, and R. C. Antweiler, 2003: The impact of a prominent rain shadow on flooding in California's Santa Cruz mountains: A CALJET case study and sensitivity to the ENSO cycle. *J. Hydrometeor.,* **4,** 1243–1264.

——, ——, and G. A. Wick, 2004: Satellite and CALJET aircraft observations of atmospheric rivers over the eastern North Pacific Ocean during the winter of 1997/98. *Mon. Wea. Rev.,* **132,** 1721–1745.

——, ——, and R. Rotunno, 2005: Dropsonde observations in low-level jets over the northeastern Pacific Ocean from CALJET-1998 and PACJET-2001: Mean vertical-profile and atmospheric-river characteristics. *Mon. Wea. Rev.,* **133,** 889–910.

——, ——, G. A. Wick, S. I. Gutman, M. D. Dettinger, D. R. Cayan, and A. B. White, 2006: Flooding on California's Russian River: Role of atmospheric rivers. *Geophys. Res. Lett.,* **33,** L13801, doi:10.1029/2006GL026689.

——, ——, G. N. Kiladis, and K. Weickmann, 2011: A multiscale observational case study of a Pacific atmospheric river exhibiting tropical–extratropical connections and a mesoscale frontal wave. *Mon. Wea. Rev.,* **139,** 1169–1189.

Schumacher, R. S., and R. H. Johnson, 2005: Organization and environmental properties of extreme-rain-producing mesoscale convective systems. *Mon. Wea. Rev.,* **133,** 961–976.

Smith, B. L., S. E. Yuter, P. J. Neiman, and D. E. Kingsmill, 2010: Water vapor fluxes and orographic precipitation over northern California associated with a landfalling atmospheric river. *Mon. Wea. Rev.,* **138,** 74–100.

Stohl, A., C. Forster, and H. Sodemann, 2008: Remote sources of water vapor forming precipitation on the Norwegian west coast at 60°N—A tale of hurricanes and an atmospheric river. *J. Geophys. Res.,* **113,** D05102, doi:10.1029/2007JD009006.

Trenberth, K. E., and C. J. Guillemot, 1996: Physical processes involved in the 1988 drought and 1993 floods in North America. *J. Climate,* **9,** 1288–1298.

Trier, S. B., and D. B. Parsons, 1993: Evolution of environmental conditions preceding the development of a nocturnal mesoscale convective complex. *Mon. Wea. Rev.,* **121,** 1078–1098.

Uccellini, L. W., 1980: On the role of upper tropospheric jet streaks and leeside cyclogenesis in the development of low-level jets in the Great Plains. *Mon. Wea. Rev.,* **108,** 1689–1696.

——, and D. R. Johnson, 1979: The coupling of upper and lower tropospheric jet streaks and implications for the development of severe convective storms. *Mon. Wea. Rev.,* **107,** 682–703.

Vasiloff, S. V., and Coauthors, 2007: Improving QPE and very short term QPF: An initiative for a community-wide integrated approach. *Bull. Amer. Meteor. Soc.,* **88,** 1899–1911.

Zhu, Y., and R. E. Newell, 1998: A proposed algorithm for moisture fluxes from atmospheric rivers. *Mon. Wea. Rev.,* **126,** 725–735.